GFZ
Helmholtz-Zentrum
POTSDAM

Originally published as:

Lucke, B., Kemnitz, H., Bäumler, R., Schmidt, M. (2013): Red Mediterranean Soils in Jordan: New insights in their origin, genesis, and role as environmental archives. - Catena, 112, 4-24

DOI: 10.1016/j.catena.2013.04.006

# Red Mediterranean Soils in Jordan: New insights in their origin, genesis, and role as environmental archives

Bernhard Lucke [a,*], Helga Kemnitz [b], Rupert Bäumler [a], Michael Schmidt [c]

[a] Friedrich-Alexander University Erlangen-Nürnberg, Institute of Geography, Kochstr. 4/4, 91054 Erlangen, Germany
[b] Helmholtz Centre Potsdam, German Research Centre for Geosciences, Section 3.1, Telegrafenberg, 14473 Potsdam, Germany
[c] Brandenburg University of Technology, Department of Environmental Planning, P.O. Box 101344, 03013 Cottbus, Germany

ARTICLE INFO

*Article history:*
Received 3 May 2012
Received in revised form 11 March 2013
Available online xxxx

*Keywords:*
Red Mediterranean Soil
Terra Rossa
Paleosol
Residue
Aeolian deposition
Isovolumetric replacement

ABSTRACT

It is disputed whether Terrae Rossae form mainly out of the bedrock residue, from allochthonous material like aerosols, or by isovolumetric replacement. Furthermore, whether they are mainly relic soils or are still forming is subject to debate. These questions were addressed by comparing the geochemistry of several limestone and basalt based Red Mediterranean Soils with Lithosols on sandstone and limestone in Jordan. The bedrock residue was included at all test sites. Paleosols and initial soils on the limestone Regolith of historic ruins delivered insights into the possible time frame of soil development. A major reduction of elements in the soils compared to bedrock could be observed for CaO in carbonaceous, $SiO_2$ in arenaceous, and $Fe_2O_3$ and MgO in basaltic rocks. All Terrae Rossae, however, are characterised by a significant increase of $SiO_2$, $Al_2O_3$, $TiO_2$, $Fe_2O_3$, $K_2O$, and a range of mainly metallic minor elements that cannot be derived from the bedrock. A reasonable explanation could be input via aeolian transfer of minerals, with clay minerals as the major carrier plus quartz. This input probably originates in Egypt and Sudan and has remained largely unchanged over long periods. Growing aridity during the Holocene has apparently increased the share of silt while clay deposition and soil development has been reduced. At some sites, metasomatic processes have contributed to soil development and might help to explain the depth of some profiles. However, formation of red soils during the Holocene seems very limited, and the Red Mediterranean Soils may represent remains of a paleolandscape.

© 2013 Elsevier B.V. All rights reserved.

## 1. Introduction

Many soils in Jordan are characterised by their red colour. Despite the ubiquitous occurrence of these soils, there is no general agreement on their origin, genesis, and age. Discussion centres particularly on their parent material: do these soils mainly represent the non-soluble residue of the underlying bedrocks, or are they largely derived from allochthonous material? Depending on which classification system is used, they are attributed to several soil groups, or are referred to as own group characterised by their colour (Red Mediterranean Soils or Terrae Rossae). The latter terminology was used mainly in older studies (e.g. Moormann, 1959; Reifenberg, 1947), which to some degree is connected to the fact that more sophisticated classification systems had not yet been developed. However, previous studies have demonstrated that the terms "Terra Rossa" and "Red Mediterranean Soil" can still be useful due to their simplicity (Lucke, 2008). "Terra Rossa" is restricted to red soils developed on limestone (Reifenberg, 1947), while "Red Mediterranean Soils" include red soils on any parent material — such as basalt or sandstone — which occur in a Mediterranean climate zone (Moormann, 1959, 23).

This paper evaluates red soils in Jordan with regard to their genesis and parent material. In order to avoid confusion and for the sake of simplicity, we largely use the soil terminology applied by Moormann (1959) and prefer the more general term "Red Mediterranean Soils" (RMS). We decided to use a comparative approach, in which soils developed on limestone are compared with soils and paleosols on basalt, sandstone and other limestone soils in the 150–500 mm annual precipitation zones. The likelihood of allochthonous deposition is evaluated by comparing the rocks and overlying soils. The location of the study sites along climatic gradients and inclusion of paleosols permits some conclusions about the role of climate for RMS development.

The prevailing explanation of the genesis of Red Mediterranean Soils on limestone was first presented by Zippe et al. (1854) and Leiningen (1930), who suggested that the red clay resembles the residue of calcareous rocks. Terrae Rossae could be the result of limestone dissolution by meteoric water, which is supported by studies from Slovakia (Bronger et al., 1984), Italy (Moresi and Mongelli, 1988), China (Ji et al., 2004a, 2004b; Shijie et al., 1999), and Turkey (Temur et al., 2009). At these locations the mineral assemblies and

* Corresponding author. Tel.: +49 91318523305; fax: +49 91318522013.
*E-mail address:* bernhard.lucke@fau.de (B. Lucke).

0341-8162/$ – see front matter © 2013 Elsevier B.V. All rights reserved.
http://dx.doi.org/10.1016/j.catena.2013.04.006

Please cite this article as: Lucke, B., et al., Red Mediterranean Soils in Jordan: New insights in their origin, genesis, and role as environmental archives, Catena (2013), http://dx.doi.org/10.1016/j.catena.2013.04.006

geochemistry of the red soils were largely identical to the non-calcareous residue of the underlying limestones.

A purely residual origin of the RMS requires the dissolution of large amounts of limestone (from several metres to many decametres, depending on the purity of the limestone) to form 1 m of soil, which appears questionable at some locations. It has been suggested that Terrae Rossae formed mainly during warm and moist periods, for example under the tropical climate conditions of the Tertiary, and are preserved as Vetusols (Meyer, 1979). However, Skowronek (1978) pointed out that the present occurrence of Terrae Rossae in Spain cannot be associated with earlier geological periods. According to him, a more recent formation of this soil type may have been possible under Garrique vegetation. In addition, there are important differences between the Terrae Rossae in the Mediterranean and current red tropical soils such as Nitisols and Ferrasols. While the latter are characterised by a high kaolinite content and leaching of silicates, the Terrae Rossae in the Mediterranean are characterised by silica enrichment and by clay mineral assemblages which are often dominated by less weathered clay minerals such as smectite.

Already Leiningen (1915) stated that the mineral assemblies of Terrae Rossae often contain allochthonous components. Yaalon and Ganor (1973) suggested that atmospheric Saharan dust settling with precipitation is the main parent material of Terra Rossa in the Near East. This theory was supported by Danin et al. (1982), who found fossil marks of lichen on limestone under a Terra Rossa, indicating that the rock had been exposed to sunlight before it was covered by soil. Studies in Indiana, U.S.A. (Ruhe and Olson, 1980), Croatia (Durn et al., 1999), the West Indies (Muhs, 2001; Muhs et al., 2007; Prognon et al., 2011), Wisconsin, U.S.A. (Stiles and Stensvold, 2008), and Spain (Muhs et al., 2010) also found that the soils were derived from allochthonous material because the geochemical composition of the investigated Terrae Rossae differed significantly from the underlying limestones. However, Jahn (1995) showed that the amount of aerosols in circumsaharian soils varied according to the climate, wind systems, and distance to the desert. In the Golan Heights, which are close to the sites investigated in this study, no more than 20% of the soil mass can be attributed to aeolian deposition.

Other studies found that both of the above mentioned parent materials, allochthonous (aeolian) sediments and residues produced by in-situ weathering of carbonate rocks, have contributed to Terra Rossa development at locations in Spain (Delgado et al., 2003; González Martín et al., 2007), Morocco (Bronger and Bruhn-Lubin, 1997), Mexico (Cabadas et al., 2010; Cabadas-Báez et al., 2010), Jordan (Lucke, 2008; Schmidt et al., 2006) and China (Feng and Zhu, 2009). According to Schmidt et al. (2006), the distribution of Terrae Rossae and Red Mediterranean Soils in Jordan indicates that these soils cannot be the exclusive product of aeolian deposition or carbonate rock weathering, but that the underlying rocks *and* allochthonous sources must play a role in their formation. In this context, a combined contribution of the bedrock and aerosols to the genesis of Red Mediterranean Soils would be present if a metasomatic genesis is assumed. This would significantly reduce the required volume of limestone bedrock for the formation of 1 m of soil. A metasomatic origin was first proposed by Blanck (1915), who suggested that the diffusion of clay-forming elements into the pores of calcareous rocks, and the precipitation of iron out of the soil–water at the rock–soil contact zone, can lead to the replacement of limestone in a pressure-driven reaction. This reaction produces acids that further dissolve calcium carbonate. The soil-forming elements would be supplied from allochthonous sources: overlying soil horizons or aeolian sediments. Using micromorphology, Merino and Banerjee (2008) identified a metasomatic front at the rock–soil transition zone of a Terra Rossa in Bloomington, Indiana, U.S.A., and developed a thermodynamic model describing the replacement reaction. Their model agrees with Blanck (1915), stating that a super-concentration of cations in the rock pore solution triggers clay mineral growth and a subsequent pressure-driven replacement of the limestone. This process also leads to a release of acids, which explains the association between Terra Rossa and karst. Similar replacement features were described for several Terrae Rossae in Jordan by Lucke et al. (2012). Close investigation of the rock–soil contact zones of different limestones with a Scanning Electron Microscope (SEM) equipped with energy-dispersive systems (EDS) made it possible to identify a jelly-like mass of apparently amorphous clay minerals that partially replaced microfossils and calcite plates (Lucke et al., 2012).

According to Blanck (1915, 1926), Terrae Rossae prevail under Mediterranean climate where soils contain little amounts of organic matter, because humus provides a “colloid” that prevents flocculation when the iron-bearing ions come in contact with the calcareous bedrock. Therefore red iron-bearing elements would be more likely to precipitate in soils of Mediterranean climates with lower humus contents. Reifenberg (1927, 1947) argued that the elements driving the growth of clay minerals were not supplied by external sources, but by ascending water from the underlying calcareous rocks. In his model, silicic acids rather than humus provide the “colloid” that prevents flocculation of sesquioxides prior to the ascension of ions into the rock pores and the soil. It is now generally assumed that the red colour of Terrae Rossae is due to strong moisture fluctuations which cause unstable ferrihydrite to form hematite (Cornell and Schwertmann, 2003). Although this process has not yet successfully been simulated in laboratory conditions, there is widespread agreement that the colour of Red Mediterranean Soils is not the result of intense weathering or very moist and warm climates in the past, but is rather typical for Mediterranean climates, and is sometimes the result of limestone dissolution, because the pre-weathered non-soluble residue might be already red. In this context, it could be shown that the rubefication process could be reversed if the soils came under a moister hydroregime, because hematite dissolves preferentially over goethite (Boero and Schwertmann, 1987). Red soil formations on Pleistocene sediments in Germany, however, demonstrate the possibility that Terra Rossa development could have taken place during the Holocene in axeric temperature areas (Schwertmann et al., 1982; Semmel, 1988).

Most soils in the Mediterranean climate zone of Jordan are dominated by red or reddish-brown colours. The distribution of soils in Jordan closely follows the climate and topography. Specific soil orders can be found within the dry and hot subtropical, subhumid–semiarid, semiarid–arid, and arid regions. In addition, the bedrock and relief position play an important role for soil distribution (Schmidt et al., 2006). The climate varies over a distance of less than 100 km from sub-humid Mediterranean conditions in the north-western part of the country to arid desert conditions in the east. The geological structure consists of layered and weakly folded limestone and sandstone, which are at some places capped by basalt flows (Bender, 1974).

Earlier investigations described a diverse pattern of Red Mediterranean Soils that seems closely connected with climate and the geology. Moormann (1959) stated that completely de-calcified Red Mediterranean Soils are only present in areas with precipitation of 600 mm or more, such as the Ajloun mountains. RMS in areas with 350–600 mm annual precipitation show increasing amounts of calcium carbonate. In areas with less than 350 mm rainfall, RMS occur only as paleosols. There are slight differences between RMS on limestone, basalt and sandstone, which are mainly reflected by the skeleton content. The skeleton content consists of limestone and chert fragments on limestones, and basalt and caliche fragments on basalt. Regarding RMS on sandstone, Moormann assumes that these are products of weathered mica-bearing sandstone that were mixed with “limestone dissolution clay” (Moormann, 1959, 23–26).

Schmidt et al. (2006) and Lucke (2008) found a similar connection between the geology and climate in the occurrence of RMS. They noted, however, that completely de-calcified RMS can not only be found in areas with 600 mm or more annual precipitation, but also

Please cite this article as: Lucke, B., et al., Red Mediterranean Soils in Jordan: New insights in their origin, genesis, and role as environmental archives, Catena (2013), http://dx.doi.org/10.1016/j.catena.2013.04.006

in areas with lower precipitation where silicified limestone prevails. In general, the character and spatial distribution of RMS on limestone is very diverse, while RMS on basalt are more homogeneous.

## 2. The study sites

In total we studied 10 soil profiles and one rock outcrop at 9 locations in Jordan (Fig. 1 and Table 1). The selection of profiles was conducted in order to obtain more precise information about the reasons behind the differences and similarities of RMS in Jordan. This was achieved by selecting sites on the one hand according to their location in different precipitation zones in northern Jordan (Fig. 1), and on the other hand by taking into account variations of bedrock (Table 1). One profile was investigated in southern Jordan in order to include sandstone bedrock which is not present in the north. All profiles are situated on level, elevated positions where fluvial addition seems unlikely. Sampling always included the bedrock.

The first profile is a Red Mediterranean Soil on basalt near the village Umm Queis in the 400 mm annual precipitation zone in northwest Jordan ("Umm Queis Basalt", samples UQ 9–23, location: N 32° 39′ 28.8″, E 35° 39′ 41.8″, location no. 1 in Fig. 1). It is located on a basalt cap which is covered by very homogeneous, deep reddish-brown soil. The basalt is an extension of the flows originating from the Djebel el-Arab in Syria during the Quaternary, approximately 700,000 years ago (Bender, 1974, El-Akhal, 2004). Between the basalt and the overlying soil, a caliche weathering crust had developed. This profile was 180 cm deep and characterised by deep drought cracks and a very uniform structure, which indicative of strong vertic dynamics (Figs. 2 and 3). Apart from breccia from the calcareous crust, the skeleton content was dominated by basalt.

The second profile, a shallow (~30 cm), grey Lithosol on Umm Rijam Chert Limestone (Moh'd, 2000) of an elevated terrace of the Wadi el-Arab near the village Umm Queis was investigated in the 400 mm annual precipitation zone ("Wadi el-Arab Lithosol", samples TZ 65–66, location: N 32° 36′ 55,5″, E 35° 39′ 25,0″, location no. 2 in Fig. 1). Apart from an Ah-horizon, the soil profile apparently consisted of crushed bedrock. This grey Lithosol was selected in order to compare less mature soil formations on limestone with the RMS.

For the third and fourth investigation sites, two RMS profiles on Umm Rijam Chert Limestone of varying hardness near the village of Yarmouk were sampled in an area with approximately 400 mm annual rainfall. The first of these developed on a karst pocket of softer limestone ("Yarmouk Limestone", samples AB 1–8, location: N 32° 42′ 54.0″, E 35° 52′ 28.8″, location no. 3 (a) in Fig. 1 and Table 1). The second profile was excavated on a hard calcareous caliche crust that capped the Umm Rijam Chert Limestone ("Yarmouk Caliche", samples AB 9–10, location: N 32° 40′ 50.7″, E 35° 52′ 35.8″, location no. 3 (b) in Fig. 1 and Table 1). These profiles were selected because they illustrate the strongly changing soil cover on limestone in the 400 mm precipitation zone in northern Jordan.

Figs. 2 and 4 show the karst pocket profile and sampling locations ("Yarmouk Limestone"). As indicated by a lithological discontinuity and increasing stone content, it seems that the upper 100 cm consist of relocated Terra Rossa material covering a paleosol that has been preserved in the karst pocket. Lucke (2008) dated this deposition event tentatively to 6880 BC. At the bottom of the profile, a 'bleached zone' was identified during another study, which is due to the occurrence of replacement processes (Lucke et al., 2012). Two samples on the slightly harder limestone next to the karst pocket were also investigated in order to ascertain whether local variations of the sedimentary rock has contributed to dissimilarities in the soil properties (samples Yar 1 Mitte, Yar Mitte unten, and Yar 5). These were evaluated for the investigation of clay minerals only.

The caliche crust was covered with a thin (~20 cm) but continuous soil cover. Apart from a high content of caliche breccia, the soil was very clay-rich and appeared strongly weathered.

In order to compare soil development with regard to time and rubefication, the fifth profile was sampled on the Umm Rijam Chert Limestone ruins of a Byzantine basilica at the archaeological site of Abila ("Abila Ruins Rendzina–Regosol", samples AB 4-1–4-4, location: N 32° 40′ 47.7″, E 35° 52′ 02.1″, location no. 4 in Fig. 1) in the 400 mm annual precipitation zone (Fig. 5). The basilica was constructed on a hilltop with Umm Rijam Chert Limestone and collapsed probably during an earthquake in 749 AD. Although the exact start date of soil formation on the present ruin surface cannot be determined exactly, it seems safe to assume that this profile represents soil development on limestone Regolith during the last 1000 years.

The sixth profile was studied in a building pit in the city of Irbid, in an area with approximately 500 mm rainfall, on Amman Silicified Limestone ("Irbid Silicified Limestone", samples I 14a–I 00, location: N 32° 31′ 53.9″, E 35° 51′ 13.7″, location no. 5 in Fig. 1). This profile is characterised by a marked change of red colour at 300 cm depth which is associated with a strong increase of chert breccia. Since the Amman Silicified Limestone is extremely rich in chert, and because there is no sign of fluvial deposition in the soil profile, we interpret this as enrichment due to weathering of the rock. This means that samples I 0 (which consist mainly of chert) to I 5 represent more or less weathered rock that has not yet turned into soil. Therefore the colour change might be explained by the strongly elevated amounts of calcium carbonate in the not yet fully disintegrated rock (Figs. 6–8).

Near the village of Amrawah, in the 300 mm annual precipitation zone near the border of the present RMS distribution, the seventh profile sampled a Red Mediterranean paleosol developed on Umm Rijam Chert Limestone that had been capped by a basalt flow (Fig. 9). The paleosol is characterised by slickensides, manganese concretions, and strong enrichment with secondary carbonates. Later, soil development resumed on top of the basalt flow (sample Am 3), but a gravel band marks an erosional event (sample Am 2). After that, RMS development resumed but with some change in the type of red colour (profile "Amrawah Limestone/Basalt", samples Am 1 — AmO 20, N 32° 40′ 42.4″, E 35° 56′ 31.7″, location no. 6 (a) in Fig. 1 and Table 1).

During a second visit in summer 2012, it turned out that part of the basalt exposed at the street opening had collapsed and revealed several pockets filled with a slightly different RMS with strong secondary carbonate concretions. Since part of this soil apparently developed inside a closed basalt cavity, it is possible that it is a soil-like weathering of the basalt due to hydrothermal water ("vulkanogenes Edaphoid", Rösner and Baumhauer, 1996), or formed due to isovolumetric replacement, which should also be possible in basalt (pers. comm. with Enrique Merino, summer 2010). Since it is not possible to assess whether the basalt cavity was completely closed, it might simply represent the remains of a paleosol that was preserved in a basalt cleft. This is indicated in at least one cavity, which is capped by gravel that was preserved directly on top of the soil pocket (Fig. 10). This pocket was sampled in order to investigate possible RMS development out of the basalt flow (samples Am BW 1 and 2, horizon (3Bsskb) in Fig. 2).

Nearby, a massive soil profile revealed a similar change of soil colour, although the basalt flow had not extended so far (profile no. 8, "Amrawah Colour Change", samples Am Fw 1–3, N 32° 40′ 42.4″, E 35° 56′ 31.7″, location no. 6 (b) in Fig. 1 and Table 1). Apparently the brighter paleosol was also present. Similar to the first Amrawah profile, a small gravel band separating two later phases of soil development could be observed (between Am Fw 1 and 2, Fig. 11). Apparently this location has seen repeated formations of Red Mediterranean Soils as a result of both the deposition of the basalt flow and tectonics (relief reversal).

The ninth profile is a series of Red Mediterranean paleosols on basalt capped by a silt-rich Regosol. It is situated near the town Umm el-Jimal in an area with approximately 150 mm mean current annual precipitation (profile "Umm el-Jimal Basalt", samples UJ 2-1–2-5, N 32° 19′ 40.3″, E 36° 21′ 40.1″, location no. 7 in Fig. 1). Three Red

Please cite this article as: Lucke, B., et al., Red Mediterranean Soils in Jordan: New insights in their origin, genesis, and role as environmental archives, Catena (2013), http://dx.doi.org/10.1016/j.catena.2013.04.006

ARTICLE IN PRESS



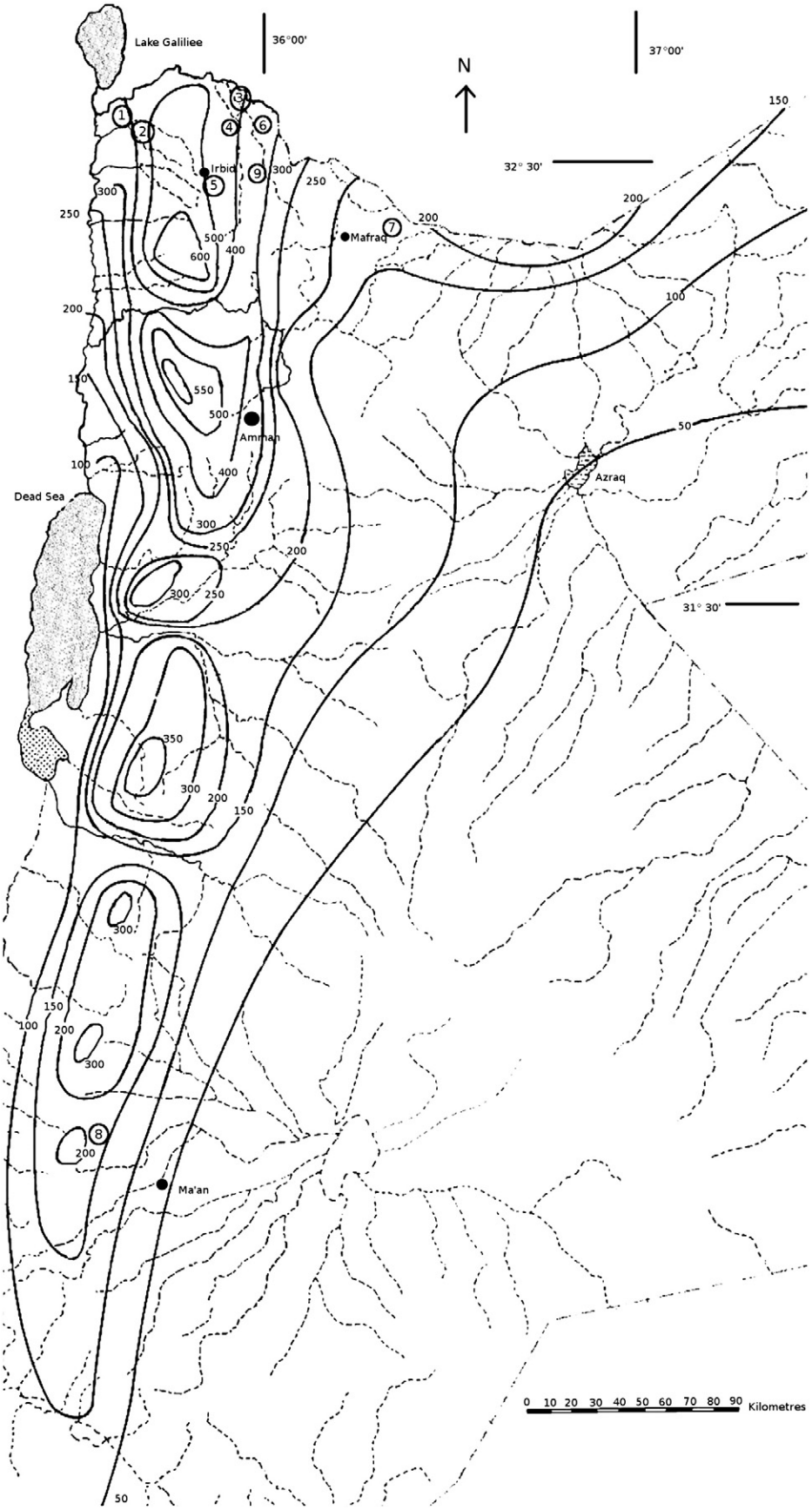


**Fig. 1.** Map showing the average annual precipitation in mm, main wadis, and the approximate locations of the sampled profiles in Jordan (see Table 1). 1: Umm Queis Basalt, 2: Wadi el-Arab Lithosol, 3: Yarmouk Limestone and Yarmouk Caliche, 4: Abila Ruins Rendzina–Regosol, 5: Irbid Silicified Limestone, 6: Amrawah Limestone/Basalt and Amrawah Colour Change, 7: Umm el Jimal Basalt, 8: Sandstone Ba'ja, and 9: Wadi Shellalah Chalk.
According to National Atlas of Jordan (1984).

Please cite this article as: Lucke, B., et al., Red Mediterranean Soils in Jordan: New insights in their origin, genesis, and role as environmental archives, Catena (2013), http://dx.doi.org/10.1016/j.catena.2013.04.006

**Table 1**
List of the sampling sites (see Fig. 1), profile names, coordinates, and bedrock units.

| Map location | Profile name | Coordinates | Average annual rainfall [mm] | Soil type | Basic bedrock unit | Detailed bedrock unit |
|---|---|---|---|---|---|---|
| 1 | Umm Queis Basalt | N 32° 39′ 28.8″<br>E 35° 39′ 41.8″ | 400 | RMS | Basalt | Alkali-olivine basalt |
| 2 | Wadi el-Arab Lithosol | N 32° 36′ 55.5″<br>E 35° 39′ 25.0″ | 400 | Lithosol | Limestone | Umm Rijam Chert Limestone |
| 3 (a) | Yarmouk Limestone | N 32° 42′ 54.0″<br>E 35° 52′ 28.8″ | 400 | RMS | Limestone | Umm Rijam Chert Limestone |
| 3 (b) | Yarmouk Caliche | N 32° 40′ 50.7″<br>E 35° 52′ 35.8″ | 400 | RMS | Limestone | Calcareous crust/caliche |
| 4 | Abila Ruins Rendzina–Regosol | N 32° 40′ 47.7″<br>E 35° 52′ 02.1″ | 400 | Regosol | Limestone | Umm Rijam Chert Limestone |
| 5 | Irbid Silicified Limestone | N 32° 31′ 53.9″<br>E 35° 51′ 13.7″ | 500 | RMS | Limestone | Amman Silicified Limestone |
| 6 (a) | Amrawah Limestone/Basalt | N 32 40′ 42.4″<br>E 35 56′ 31.7″ | 300 | RMS | Limestone and basalt flow | Umm Rijam Chert Limestone |
| 6 (b) | Amrawah Colour Change | N 32 40′ 42.4″<br>E 35 56′ 31.7″ | 300 | RMS | Limestone | Umm Rijam Chert Limestone |
| 7 | Umm el-Jimal Basalt | N 32° 19′ 40.3″<br>E 36° 21′ 40.1″ | 150 | RMS | Basalt | Fahda Basalt and Abed Basalt |
| 8 | Sandstone Ba'ja | N 30° 24′ 56,3″<br>E 35° 27′ 40,2″ | 150 | Lithosol | Sandstone | Kurnub Sandstone |
| 9 | Wadi Shellalah Chalk | N 32° 35′ 24″<br>E 35° 57′ 17.6″ | 300 | Chalk exposure | Chalk | Wadi Shallala Chalk |

Mediterranean paleosols were identified (Figs. 2 and 12). The initial paleosol observable in this sample had been capped by a basalt flow, after which red soil development resumed. This soil was then eroded before being covered by renewed red soil development. Finally a silty Regosol capped the RMS paleosols. The Regosol possibly resembles a Loess cover (Cordova, 2007). The basalt originated at the Djebel el Arab in Syria, and it seems likely that the lower paleosol developed on Abed Olivine-Phyric Basalt from the Miocene (not sampled), which was capped during the Holocene–Pliocene by Fahda Vesicular Basalt (sample UJ 2 basalt 1). During the Quaternary, formation of the Red Mediterranean Soils stopped and approximately 20 cm of probably aeolian material was deposited which formed the silty Regosol on top (sample UJ 2-1). The upper part of the red paleosol below the aeolian layer (20–70 cm) is characterised by firm aggregates and many secondary carbonates (sample UJ 2-2), while the deeper part (70–110 cm) has very hard prismatic aggregates and many secondary carbonates as well. There is a sharp change in 110 cm depth, characterised by a different prismatic structure and the appearance of gypsum crystals, which indicates that there is second red paleosol (sample UJ 2-4) which had developed on the basalt cap. The oldest red paleosol (sample UJ 2-5) between the two basalt flows was characterised by many hard gypsum crystals which in some cases reach fist size.

The tenth profile is a Lithosol in southern Jordan which was investigated in order to compare soil development on sandstone bedrock (Fig. 13). The profile is situated near the ancient sites of Petra and Ba'ja with approximately 150 mm annual precipitation ("Sandstone Ba'ja", samples Sandplateau 1–4, location: N 30° 24′ 56,3″, E 35° 27′ 40,2″, location no. 8 in Fig. 1). Although it does not resemble one of Moormann's (1959) Red Mediterranean Soils on sandstone (which occur mostly in depressions), it is located on the same bedrock.

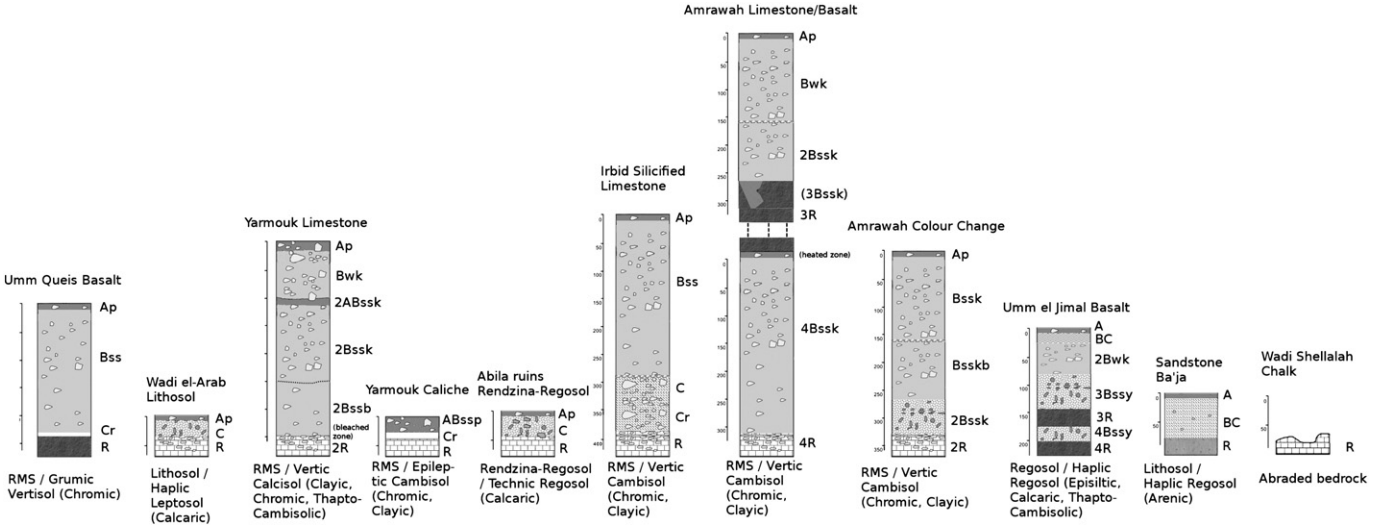


**Fig. 2.** Drawing of all sampled profiles. "RMS" stands for "Red Mediterranean Soil".
The soils were classified according to the system used in the article and according to WRB (2007). The soil horizons were designated according to USDA (2005).


**Fig. 3.** Sampling the Red Mediterranean Soil on basalt near the village Umm Queis. Each mark on the metre represents 10 cm.

Finally, a sample was obtained from a chalk exposure in the north-eastern part of the study area at the slopes of Wadi Shellalah, which were strongly eroded — possibly partially due to wind erosion — and might contribute to local dust emissions. It was analysed for its content of clay minerals only (sample "Wadi Shellalah Chalk", N 32° 35′ 24″, E 35° 57′ 17.6″, location no. 9 in Fig. 1).

## 3. Methods

Soils were analysed for Redness Rating (RR), pH, electrical conductivity, $CaCO_3$-content, soil development indices based on iron oxides and aluminium, magnetic susceptibility, texture, clay mineral content, and total element content. These results allow for a comparison of soil development from a soil genetic point of view, and to assess inheritance according to stable element-ratios (Lucke, 2008).

For the collection of soil samples, freezer bags were filled from a ca. 5 cm thick strip in the middle of the identified layers/horizons (from large horizons sometimes several samples were taken in regular intervals). The samples were air-dried for 48 h at 40 °C and then passed through a 2 mm sieve. The remaining material, i.e. that with a particle diameter >2 mm (skeleton content) was weighed to determine the mass fraction and archived, and all further analyses conducted with the material with a particle diameter <2 mm. Colour was determined in the laboratory under standardised light, using the Munsell soil colour chart. The Redness Rating (RR) was computed with the dry samples according to Hurst (1977) (the index becomes smaller with increasing redness). Electrical conductivity was measured with a GMH 3410 conductivity metre by Greisinger electronic in a soil:water solution of 1:5 (according to Schlichting et al., 1995). Contents of $CaCO_3$ were determined using a LecoTrueSpec C/N-analyser in doubles before and after ignition for 2 h at 430 °C. Pedogenic oxides were extracted with sodium dithionite at room temperature according to Holmgren (Schlichting et al., 1995), and the iron and aluminium contents measured with atomic absorption spectrometry (M-series by Unicam, thermo-flame-spectrometer). Weakly crystallised pedogenic oxides were extracted in the dark using buffered (pH 3.25) oxalate-solution according to Schwertmann (Schlichting et al., 1995). Their iron and aluminium contents were determined with the atomic absorption spectrometer (AAS), too. The total elemental content of the samples was examined using a wavelength-dispersive sequence spectrometer, type

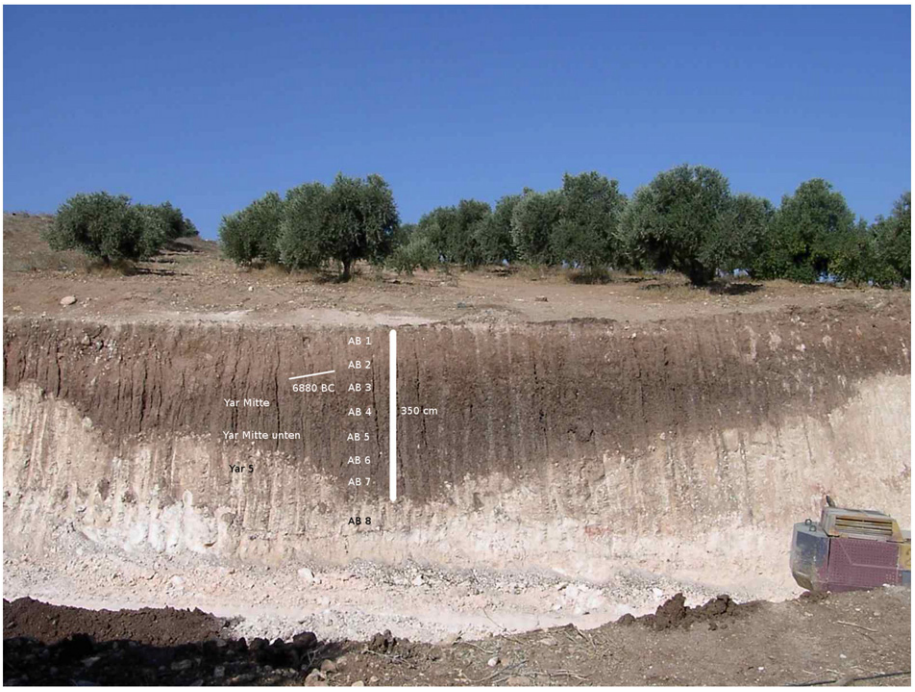


**Fig. 4.** Sampling the Red Mediterranean Soil on limestone near the village of Yarmouk.

Please cite this article as: Lucke, B., et al., Red Mediterranean Soils in Jordan: New insights in their origin, genesis, and role as environmental archives, Catena (2013), http://dx.doi.org/10.1016/j.catena.2013.04.006

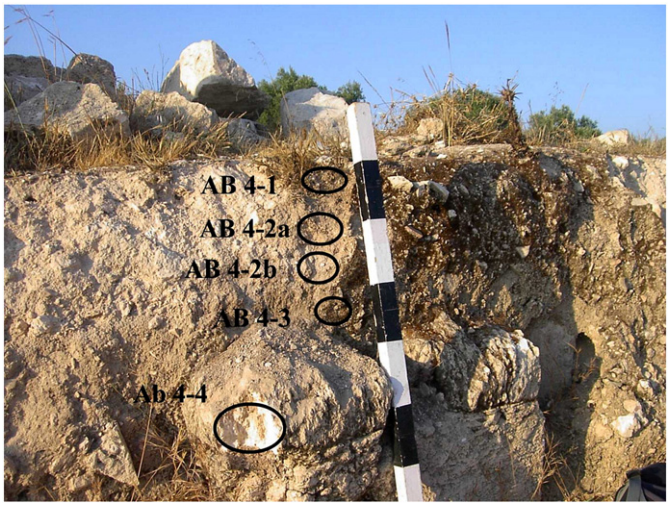


**Fig. 5.** Sampling the initial Rendzina–Regosol developed on limestone Regolith on the ruins of the area A basilica of the ancient site Abila. Each mark on the metre represents 10 cm.

PW 2400 according to DIN 51001 (2003). The specific susceptibility χ was determined using a Kappabridge KLY-3S magnetic susceptibility metre (875 Hz), using the sieved but otherwise untreated fine soil <2 mm.

Particle sizes were analysed after removing $CaCO_3$ with 10% hydrochloric acid (until no visible reaction occurred any more). The hydrochloric acid (HCl) was then washed out and those samples with $C_{org} > 2\%$ were treated with 30% hydrogen peroxide ($H_2O_2$) in a warm waterbath (~50 °C), until no further visible reaction occurred. The hydrogen peroxide was then evaporated and the samples dispersed using sodium hexametaphosphate ($Na_4P_2O_4$). Wet sieving determined the sand fractions (according to DIN 19683, 1973), while the smaller particles were analysed using sedimentation analysis according to Köhn (Schlichting et al., 1995).

Clay minerals were determined using a D 5000 X-ray diffractometer. The examination focused on the angle range of 2–33° 2θ, and the approximate quantification of clay minerals was conducted according to the Rietveld method (Rietveld, 2010) which statistically eliminates amorphous minerals (assuming that all are crystalline). For preparation of the samples, especially the rock samples, 0.11 M HCl was used to remove calcium carbonate under constant monitoring of the pH in order to exclude alterations of the clay minerals due to acid treatment. In order to assure the suitability of the method several test runs were conducted (Lausser, 2010).

Based on the total elemental content of the samples, several ratios were calculated: Ti/Zr, Ba/Sr, and a base accumulation index ($SiO_2 + TiO_2 + Al_2O_3 + Fe_2O_3 + MnO + MgO + Na_2O + K_2O$)/CaO. The Ti/Zr ratio seems the best available index for assessment of inheritance, and the barium/strontium relationship is a weathering index based on the comparison of a stable with an unstable element. Compared with the parent material, increased weathering of the soil should lead to a depletion of the less stable elements and the accumulation of the more stable ones (Retallack, 2001). Weathering indices are problematic in areas with a negative water balance such as Jordan, since the frequent drying of soils may lead to accumulation of cations, which are otherwise quickly washed out. Nevertheless the Ba/Sr-index was determined and the results showed that Ba was enriched in most soils, and Sr mostly depleted. A base-accumulation-index was calculated involving all ions that showed frequent enrichment, divided by calcium which alone is depleted in most soils.

Last but not the least, the contents of major and minor elements were recalculated for the limestone bedrock samples AB 8, AB 10, and I 0, by subtracting the maximum possible mass contents of $CaCO_3$ calculated according to the CaO-content from total element analysis under the assumption that the results refer only to the $CaCO_3$-free residue, thus eliminating the 'diluting' effect of limestone $CaCO_3$.

**Fig. 6.** The Red Mediterranean Soil on silicified limestone revealed by a construction pit in the city of Irbid. Each mark on the metre represents 10 cm. The picture was first published in Lucke (2008, 45) and is reprinted with permission of Akademikerverlag.

Please cite this article as: Lucke, B., et al., Red Mediterranean Soils in Jordan: New insights in their origin, genesis, and role as environmental archives, Catena (2013), http://dx.doi.org/10.1016/j.catena.2013.04.006

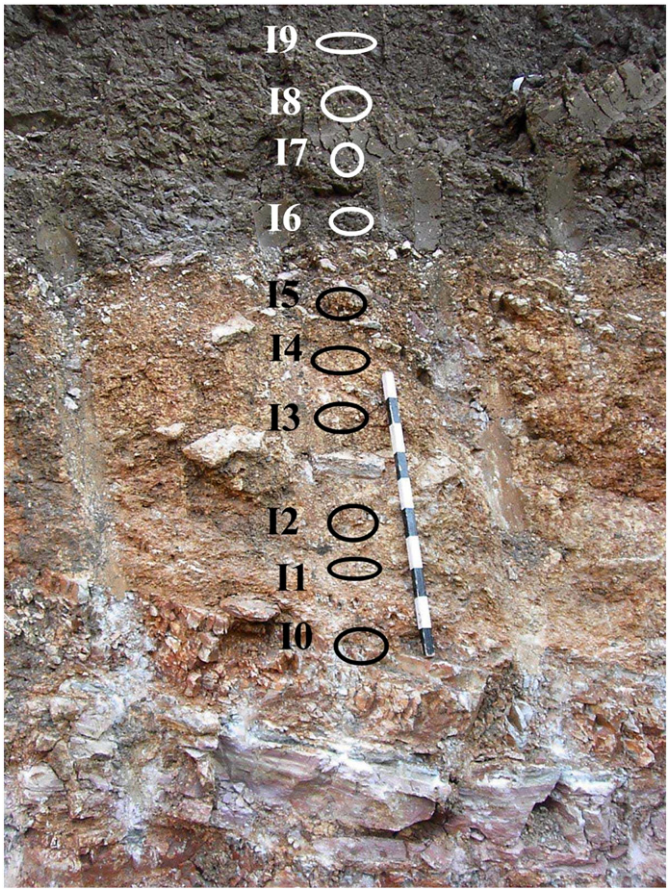


**Fig. 7.** Sampling the lower part of the Red Mediterranean Soil on silicified limestone near Irbid. Each mark on the metre represents 10 cm.

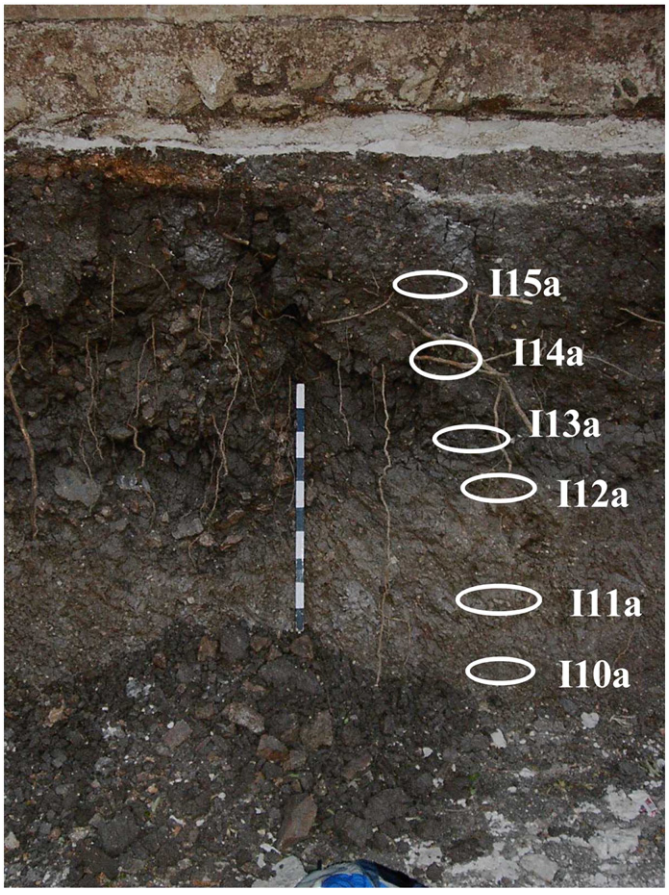


**Fig. 8.** Sampling the upper part of the Red Mediterranean Soil on silicified limestone near Irbid. Each mark on the metre represents 10 cm.

## 4. Results

### *4.1. General soil development*

The general soil analyses show a partially diverse and partially homogeneous picture of soil development (Table 2). The weathering intensity of the RMS, as expressed by RR, $CaCO_3$, Fe(d), aluminium content, Ba/Sr and the base accumulation index is highest in the Irbid and Yarmouk caliche profile, and in the Amrawah paleosol. It seems that soil development intensity is not as simply related to climate as proposed by Moormann (1959): the bedrock, and possibly the age, of the RMS seem to play a role too.

In this context, it seems unlikely that the very pure Yarmouk caliche contributed much residue to the formation of the overlying RMS. This is further supported by the quite different Ti/Zr values of the soil and bedrock. It is interesting to note that the Ti/Zr ratios of most investigated profiles differ clearly between the soil and underlying rock, but are similar throughout each profile. Exceptions are the Lithosol on sandstone and the Rendzina–Regosol on the Abila ruins which seem to reflect the bedrock.

The Ti/Zr values of the RMS on basalt near Umm Queis and the upper red paleosol in Umm el Jimal are similar. It is noteworthy that only the RMS on limestone at the Yarmouk-profile has similar values. Compared to the other RMS on limestone, the Yarmouk-profile contrasts not only with regard to the Ti/Zr-ratio, but also regarding soil development intensity which is most pronounced at the bottom of the Yarmouk profile, whereas the other soils have their strongest weathering intensity in the topsoil.

The Lithosol on sandstone and the Rendzina–Regosol on the ruins of Abila show very weak soil development and, according to the analyses, merely represent crushed bedrock. This is not surprising since the sandstone Lithosol is easily eroded and located in a zone with very little precipitation. The Rendzina–Regosol on the Abila ruins indicates that there was no RMS neo-formation out of limestone Regolith within the past 1000 years — in fact the profile reveals little soil formation at all. In this context, the similar Ti/Zr ratios of bedrock and soil support the impression that the Lithosols consist of crushed bedrock. It seems that the Wadi el-Arab Lithosol is probably older than 1000 years since a slightly stronger pedogenesis can be observed there. This might also be the reason for a higher Ti/Zr-ratio in the Wadi el-Arab.

This difference is even more pronounced in the RMS soils, although some caution has to be taken. Since the sedimentary rock layers which may have provided the residue for soil formation may have been completely weathered, there is no safe information about the former rock composition. It cannot be excluded, therefore, that titanium-rich sandy interlayers caused the increased Ti/Zr values in the limestone RMS. However it is also possible that external sources contributed allochthonous material to the formation of these soils which caused the increase of the Ti/Zr-ratio.

Similarly, the decrease of the Ti/Zr ratio of the RMS on basalt could be taken as indication for allochthonous materials containing less titanium than the basalt bedrock. However, again caution has to be taken. Zircon, one of the most resistant minerals against any type of weathering, should always be enriched during pedogenesis. In basaltic rocks, zircon is rather rare, but is more prevalent than in limestone, where it will nearly exclusively be found in sandy interlayers. Titanium, on the other hand, is an element of several major mineral components in basic rocks, such as rutile, biotite, amphiboles, pyroxenes, and magnetite. Only the Ti-rich magnetite shows a high weathering resistivity. Therefore, the weathering profile of a basaltic soil is characterised by

Please cite this article as: Lucke, B., et al., Red Mediterranean Soils in Jordan: New insights in their origin, genesis, and role as environmental archives, Catena (2013), http://dx.doi.org/10.1016/j.catena.2013.04.006


**Fig. 9.** The Red Mediterranean Soil on limestone capped by a basalt flow and another Red Mediterranean Soil near the village of Amrawah in 2005. Each mark on the metre represents 10 cm.
The picture was first published in Lucke (2008, 46) and is reprinted with permission of Akademikerverlag.

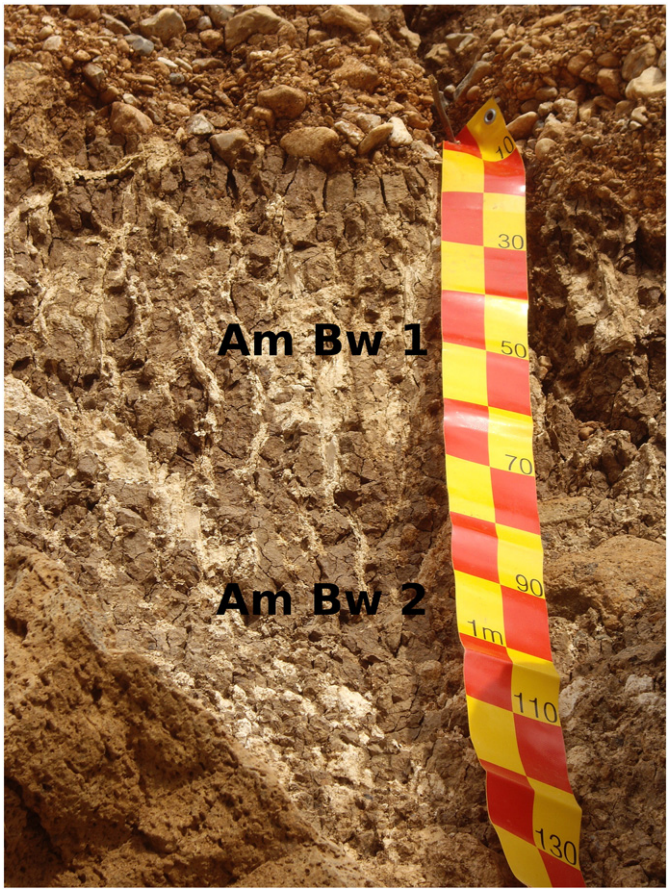


**Fig. 10.** RMS soil pocket in the basalt flow near Amrawah (see Fig. 9), capped by fluvial gravels, and revealed due to a partial collapse of the basalt exposure in 2012.

decreasing Ti contents, even if some Ti might have been added by aeolian influx of phyllosilicates like muscovite, biotite, or chlorite.

However, it seems safe to assume that the contribution of basalt weathering to soil development should result in slightly elevated Ti/Zr-ratios, which is the case at Umm Queis and Umm el Jimal, but not at the basalt flow near Amrawah. This is further indicated by the Amrawah Colour Change profile, which is close to the basalt flow, but was not affected and shows a nearly identical composition to the Amrawah RMS at the basalt flow. Therefore, it seems likely that basalt weathering did not contribute significantly to soil development near Amrawah, but to some degree near Umm Queis and Umm el-Jimal. In this context, the elevated Ti/Zr-ratios in the Yarmouk Limestone profile could be taken as indication of the presence of volcanic material from the Cretaceous that had been deposited inside the limestone rocks, as suggested earlier by Lucke et al. (2012).

In the RMS on limestone, the content of $CaCO_3$ seems a good indicator for the assessment of weathering intensity, since the values are largely in agreement with both the field interpretation and the Ba/Sr and base accumulation ratios. The absolute amount of Fe(d) seems to be a good indicator for pedogenesis in all investigated profiles, including the RMS on basalt, whereas the Fe(d/t) ratio seems not to work well. This could be connected with the extraction of pre-weathered iron from primary $CaCO_3$ in the limestone soils (Lucke, 2008), and with the possibility that pedogenic iron in the sandstone soil is largely derived from the deposition of pre-weathered clay with aerosols.

According to the analyses, the aeolian cover of the Umm el-Jimal red paleosol sequence is not reflected by a drop of soil development intensity. In fact, the opposite is the case: nearly all indicators of the extent of soil development increase in the top layer, only the texture shows a limited increase of silt. This means that the probably aeolian sediments at Umm el-Jimal apparently consist of pre-weathered material rich in silt and relatively poor in calcium carbonate.

Reviewing texture, it should be noted that the values have to be interpreted with caution since the dissolution of $CaCO_3$ with HCl during pre-treatment means that the texture of soils rich in calcium carbonate might to some degree reflect the grain sizes of the insoluble residue. However, the values show a tendency of increasing silt contents towards the east, which might reflect the influence of aeolian sediments similar to the top layer of the Umm el-Jimal RMS sequence. In contrast, the western and southern locations, such as the RMS on basalt near Umm Queis, the Lithosol in Wadi el Arab, and the Lithosol on sandstone near Ba'ja have very low silt contents. The texture of the sandstone soils seems largely inherited from the rock, while the exceptional high clay values of the RMS on basalt near Umm Queis are in agreement with the strong vertic properties of the profile.

The limestone profile near the village of Yarmouk is of central importance. Only at this site could a 'bleached zone' in contact with bedrock be identified (Lucke et al., 2012). This is in agreement with the exceptional increase of soil development intensity towards the bottom of the RMS, which had initially been assumed to be connected with the obvious fluvial deposition of allochthonous material in the upper 100 cm of the profile, but might now be attributed to isovolumetric replacement. Comparison with the very closely located RMS on caliche reveals some differences: a lower Ti/Zr ratio, which points to the absence of volcanic contributions in the caliche RMS, but higher soil development intensity. However, the highest soil development intensity is present in the RMS on silicified limestone near Irbid.

Please cite this article as: Lucke, B., et al., Red Mediterranean Soils in Jordan: New insights in their origin, genesis, and role as environmental archives, Catena (2013), http://dx.doi.org/10.1016/j.catena.2013.04.006

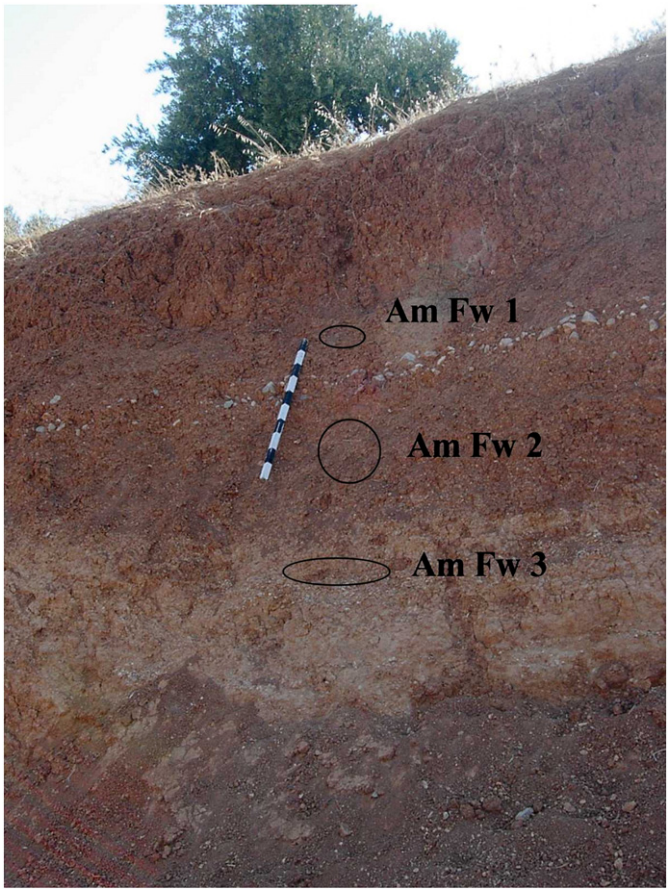


**Fig. 11.** The sampled colour change in a RMS without basalt deposition near the village of Amrawah. Each mark on the metre represents 10 cm.
The picture was first published in Lucke (2008, 47) and is reprinted with permission of Akademikerverlag.

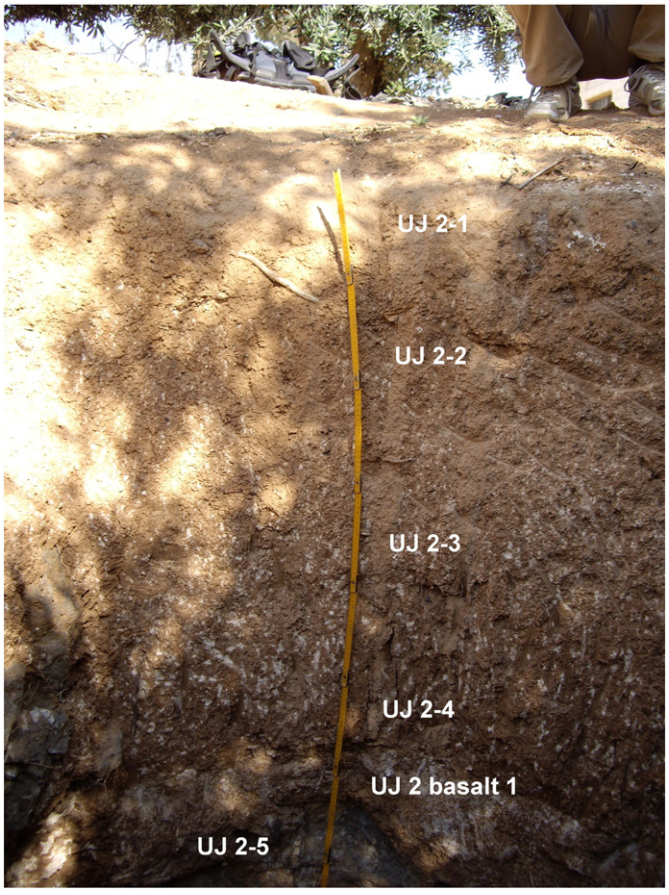


**Fig. 12.** The Regosol and two RMS paleosols until the first basalt flow near the village of Umm el Jimal. The metre represents 2 m.

### 4.2. Distribution of major elements

Table 3 and Fig. 14 illustrate the distribution of major elements in the investigated profiles. The RMS on basalt and the Lithosol on sandstone both show a minor depletion of $SiO_2$ compared to the basalt and sandstone bedrocks. This is also true for most other major elements of the soils on these rocks, which points towards in-situ genesis out of the bedrock. In this context, the increase of CaO and decrease of most other major elements in the Rendzina–Regosol on the ruins of Abila confirms the earlier picture of very weak — if any — soil development. In contrast, there are strongly increasing values of $SiO_2$ and decrease of CaO in all other limestone soils. The RMS on limestone, as well as the Lithosol in Wadi el-Arab, are characterised by major accumulation of $SiO_2$, but also $Al_2O_3$, $Fe_2O_3$, $K_2O$, and $TiO_2$, which can hardly be explained by accumulation due to bedrock weathering. CaO, in contrast, is strongly depleted in the limestone RMS which points to dissolution of the bedrock and external additions.

The recalculation of major element contents after subtraction of $CaCO_3$ in the limestone bedrock samples AB 8 and AB 10 produced values for most elements, in particular for $Al_2O_3$ and $SiO_2$, which let it seem possible that the soil represents the bedrock residue. However, a strong, selective depletion of magnesium during soil genesis would have to be postulated. Due to the small content of calcium carbonate in the Amman silicified limestone of sample I 0, the recalculation of this sample however cannot explain the enrichment of most major elements in the soil of the Irbid Silicified Limestone profile.

Again, while most RMS are most strongly enriched in the topsoil, the trend is opposite in the Terra Rossa developed on limestone near the village Yarmouk; at the lowermost soil layer above the bedrock this soil first shows a sharp increase of elements not typical in carbonaceous rocks, and subsequently a weak, but gradual depletion of these elements with decreasing depth. Ca, in contrast, was firstly drained off with weathering, but shows an apparent gradual increase. The increase of calcium carbonate in its upper part must be connected with a deposition of calcareous material as had already been indicated by the field evidence.

It can be summarised that:

- A major reduction of elements can be observed only for those elements in the source rocks that have a base level significantly higher than the mean composition of a mature red soil. These are mainly CaO in carbonaceous, $SiO_2$ in arenaceous, and $Fe_2O_3$ and MgO in basaltic rocks. If Ca plays a major role in a source rock composition as for instance in basalt or a carbonate, it will always be leached during the process of red soil formation. In Ca-poor rocks alone (sandstone in our study), a weak increase of CaO can be observed compared to the base level.
- Regarding the Red Mediterranean Soils on limestone, their formation seems primarily related to the intensity of calcium carbonate leaching.
- Similarly, it can be argued that increasing CaO contents across all those red soils not developed on limestone require the addition of external calcium-rich material. This may point to local, Ca-enriched dust sources.
- The RMS on basalt are characterised by a rather constant composition from bedrock to the topsoil. The basaltic rock provides nearly all basic ingredients — major and minor elements — for RMS formation. According to the major element contents, bedrock weathering can explain this soil formation.

Please cite this article as: Lucke, B., et al., Red Mediterranean Soils in Jordan: New insights in their origin, genesis, and role as environmental archives, Catena (2013), http://dx.doi.org/10.1016/j.catena.2013.04.006


**Fig. 13.** The Lithosol on sandstone near the site of Ba'ja. The metre represents 1 m.

- A similar relationship between bedrock and soil can be concluded for the Lithosols developed on sandstone near Ba'ja and limestone debris at Abila, showing a low extent of pedogenesis.
- The comparison between red palaeosols that were buried either by basalt flows or silty sediments yields no significant differences.

Reviewing the distribution of $SiO_2$, $Al_2O_3$, $TiO_2$, and CaO, some remarkable trends can be observed (Fig. 15). Apart from the rock samples from basalt and sandstone, the chert bedrock of the silicified limestone below the Irbid RMS (sample I 0), and the Ba'ja Lithosol on the sandstone, the contents of these elements are clearly correlated. If the basalt rocks, the sandstone and the Ba'ja Lithosol on the sandstone are ignored, the resulting linear functions allow for the prediction of $SiO_2$, $Al_2O_3$, $TiO_2$, and CaO content in a RMS — either on limestone or basalt — with high confidence. In the case of $SiO_2$ and $Al_2O_3$ (assuming that the above mentioned elements are mainly part of phyllosilicates, i.e. clay minerals), it is possible to express the relationship of these elements for the investigated RMS with the formula: $SiO_2\ (\%) = 3.3989 * Al_2O_3\ (\%) + 1.7274$, with an $R^2$ value (coefficient of determination) of 0.91, which means that 91% of the variation can be explained by this linear extrapolation. In the case of the correlation between $Al_2O_3$ and $Fe_2O_3$ in the investigated RMS, the coefficient of determination reaches 99%, which probably reflects the dominance of montmorillonite or nontronite. It is remarkable that this includes the limestone and their residue. Also striking is the strong correlation between the $SiO_2$ and $TiO_2$ contents (explains 98% of the variation), which is stronger than the correlation between $Fe_2O_3$ and $TiO_2$ (explains 96% of the variation), considering a common origin from igneous rocks. $TiO_2$ may probably have been brought with clay minerals. Hence, the enrichment of $SiO_2$, $Al_2O_3$ and $TiO_2$ in the RMS might reflect mainly the accumulation of clay minerals. It can be concluded that the residue of the calcareous rocks containing these elements also consist essentially of clay minerals.

### 4.3. Distribution of minor elements

Table 4 and Fig. 16 show the distribution of minor elements. In contrast to the major elements, there is no clear tendency or correlation of enrichment or depletion between the minor elements in the investigated soils and rocks. Again, the RMS on basalt seemingly mirror the bedrock composition, with subordinated reduction of some elements, such as Sr which is often leached with $CaCO_3$. Some metals, such as V, Zn, Cu, and Co, appear to be depleted as well, whereas Zr, Ba, Rb, Ce, and Th are enriched. The slight fluctuations throughout the profiles seem to reflect common soil development processes: weathering of the original igneous minerals, and fixation of minor elements in new (clay) minerals formed during pedogenesis.

In contrast, the RMS on limestone, as well as the Lithosol on sandstone show a strong enrichment of basically all minor elements except Sr. In this context, the soil samples with strongest weathering (see Table 2) also show the strongest enrichment of minor elements. The depletion of Sr in the limestone soils correlates to some degree linearly with the $CaCO_3$-content (explains 57% of the variation), indicating the connection of Sr with calcium carbonate.

The recalculation of minor element contents after subtraction of $CaCO_3$ in the limestone bedrock samples AB 8 and AB 10 produced very high values for most elements which appear unlikely. Compared to the basalt bedrocks, where a 'diluting' effect of $CaCO_3$ on the bedrock residue should not be indicated, an extraordinary strong depletion of most minor elements during pedogenesis of the limestone soils would have to be postulated, which is not reasonable.

The significant enrichment of minor elements like Ce, Co, Cr, Rb, V, Zr, and partly Ba and Pb cannot be explained by weathering from calcareous rocks since the same element distribution is present in the RMS on basalt, as well as in the Wadi el-Arab Lithosol and the sandstone Lithosol. In all cases, the results reflect the geochemistry of a soil rich in clay minerals, suggesting allochthonous, aeolian additions. Enrichment of these minor elements is discernible even in the Rendzina–Regosol on the Abila ruins, which is thought to mirror an immature stage of soil formation as its elemental composition is largely identical to the calcareous rocks.

To summarize:

- Considering the absolute amounts of minor elements, it is remarkable that the RMS on limestone and basalt are largely identical. The enrichment of minor elements seems unconnected to the bedrock, rather it merely reflects the intensity of pedogenesis (and thus, probably the age) of the respective soils.
- It is remarkable that the silty layer capping the RMS paleosols near Umm el Jimal (sample UJ 2-1) is not distinguishable from the RMS soil samples. In the context of the laboratory analyses, the structural differences due to the increase of silt seem less important. Thus this soil horizon might represent a degraded A-horizon of a RMS on basalt, which was strongly enriched with silty additions very similar to the main parent material of the RMS.
- A reasonable explanation for the origin of this silty layer could be incomplete basalt weathering combined with aeolian input of clay minerals as major carrier minerals plus quartz. This is an ongoing process with a more or less constant supply from the same external source region, but a significantly larger share of silt when climate changed towards aridity.

### 4.4. Clay mineralogy

Table 5 summarises the clay mineralogy of the investigated soil profiles. In addition, it presents the sample "Wadi Shellalah Chalk", taken from a strongly eroded chalk exposure near the Wadi Shellalah

Please cite this article as: Lucke, B., et al., Red Mediterranean Soils in Jordan: New insights in their origin, genesis, and role as environmental archives, Catena (2013), http://dx.doi.org/10.1016/j.catena.2013.04.006

**Table 2**
Results of general soil analyses. The bedrock samples were marked with colour: orange for the calcareous rocks, grey for basalt, yellow for sandstone, and light red for weathering crusts of the rocks.

| No. | Sample legend/ depth | RR | pH | Conductivity [µS/cm] | $CaCO_3$ % | Fed [mg/g] | Fe(d/t) | Alo [mg/g] | Ald (mg/g) | χ [1/kg] *E–3 | Clay % | Silt % | Sand % | Skeleton % | Ti/Zr | Ba/Sr | Base accumulation index |
|---|---|---|---|---|---|---|---|---|---|---|---|---|---|---|---|---|---|
| | Yarmouk Limestone | | | | | | | | | | | | | | | | |
| 1 | AB 1 (50 cm) | 29 | 8.2 | 160 | 44 | 10.3 | 0.32 | 1.2 | 0.6 | 120 | 69 | 22 | 9 | 30 | 30 | 1.7 | 1.7 |
| 2 | AB 2 (100 cm) | 29 | 8.1 | 194 | 48 | 7.5 | 0.24 | 1.2 | 0.5 | 116 | 68 | 21 | 11 | 18 | 29 | 1.6 | 1.5 |
| 3 | AB 3 (150 cm) | 11 | 8.2 | 129 | 32 | 13.3 | 0.34 | 1.6 | 0.9 | 157 | 77 | 21 | 2 | 10 | 29 | 2.2 | 2.6 |
| 4 | AB 4 (200 cm) | 15 | 8.3 | 133 | 30 | 9.3 | 0.23 | 1.5 | 0.8 | 162 | 77 | 21 | 2 | 12 | 30 | 2.1 | 3.0 |
| 5 | AB 5 (250 cm) | 15 | 8.4 | 154 | 22 | 8.8 | 0.18 | 1.8 | 0.9 | 182 | 76 | 23 | 1 | 10 | 31 | 2.6 | 4.8 |
| 6 | AB 6 (300 cm) | 18 | 8.3 | 247 | 12 | 13.6 | 0.26 | 2.2 | 0.9 | 211 | 77 | 19 | 4 | 5 | 32 | 2.9 | 7.7 |
| 7 | AB 7 (350 cm) | 15 | 8.3 | 236 | 11 | 13.4 | 0.24 | 2.1 | 1.0 | 238 | 78 | 19 | 3 | 2 | 30 | 2.1 | 7.6 |
| 8 | AB 8 (bedrock) | | | | 90 | | | | | | | | | | 11 | 0.1 | 0.2 |
| | Yarmouk Caliche | | | | | | | | | | | | | | | | |
| 9 | AB 9 (10 cm) | 8 | 8.4 | 112 | 5 | 14.6 | 0.28 | 2.6 | 1.4 | | 75 | 23 | 2 | 4 | 26 | 4.2 | 13.5 |
| 10 | AB 10 (bedrock) | | | | 92 | | | | | | | | | | 14 | 0.2 | 0.1 |
| | Irbid Silicified Limestone | | | | | | | | | | | | | | | | |
| 11 | I 14a (60 cm) | 15 | 8.2 | 92 | 3 | 23.2 | 0.46 | 1.9 | 1.7 | | 66 | 29 | 5 | 5 | 23 | 3.5 | 29.6 |
| 12 | I 9 (200 cm) | 29 | 8.0 | 180 | 11 | 11.9 | 0.23 | 1.0 | 1.3 | | 66 | 29 | 5 | 10 | 27 | 3.2 | 11.5 |
| 13 | I 4 (290 cm) | 47 | 8.4 | 242 | 67 | 7.5 | 0.30 | 0.3 | 0.6 | | 55 | 3 | 42 | 44 | 40 | 0.7 | 0.7 |
| 14 | I 0 (bedrock) | | | | 5 | | | | | | | | | | 16 | 12.7 | 37.1 |
| | Abila Ruins Rendzina-Regosol | | | | | | | | | | | | | | | | |
| 15 | AB 4-1 (5 cm) | 53 | 8.7 | 163 | 73 | 3.3 | 0.25 | 0.7 | 0.3 | | 48 | 24 | 28 | 52 | 24 | 0.7 | 0.5 |
| 16 | AB 4-2a (8 cm) | 47 | 8.4 | 126 | 81 | 2.1 | | 0.5 | 0.4 | | 71 | 21 | 8 | 10 | | | |
| 17 | AB 4 -2b (19 cm) | 160 | 8.3 | 92 | 74 | 3.5 | 0.32 | 0.3 | 0.2 | 55 | 65 | 22 | 14 | 36 | 25 | 0.7 | 0.4 |
| 18 | AB 4-3 (28 cm) | 61 | 8.7 | 103 | 72 | 3.6 | 0.16 | 0.6 | 0.3 | | 42 | 25 | 33 | 23 | 25 | 0.7 | 0.5 |
| 19 | AB 4-4 (limestone) | | | | | | | | | | | | | | 27 | 3.8 | 0.1 |
| | Wadi el-Arab Lithosol | | | | | | | | | | | | | | | | |
| 20 | TZ 65 (10 cm) | 50 | 7.8 | 220 | 61 | 5.7 | 0.33 | 0.2 | 0.2 | | 25 | 11 | 64 | 55 | 24 | 0.6 | 1.0 |
| 21 | TZ 66 (bedrock) | | | | | | | | | | | | | | 18 | 0.3 | 0.1 |
| | Umm Queis Basalt | | | | | | | | | | | | | | | | |
| 22 | UQ 9 (10 cm) | 18 | 8.1 | 116 | 13 | 11.2 | 0.22 | 1.8 | 1.0 | 147 | 89 | 7 | 4 | 4 | 33 | 3.0 | 6.9 |
| 23 | UQ 13 (90 cm) | 29 | 8.4 | 145 | 15 | 11.2 | 0.21 | 2.0 | 1.0 | | 87 | 8 | 6 | 6 | 33 | 3.0 | 6.8 |
| 24 | UQ 21 (160 cm) | 23 | 8.2 | 165 | 13 | 11.4 | 0.21 | 2.0 | 0.9 | | 88 | 7 | 5 | 1 | 32 | 2.9 | 7.3 |
| 25 | UQ 23 (caliche) | | | | | | | | | | | | | | 8 | 0.2 | 0.0 |
| 26 | Basalt UQ (bedrock) | | | | | | | | | | | | | | 80 | 0.9 | 6.7 |
| | Umm el-Jimal Basalt | | | | | | | | | | | | | | | | |
| 27 | UJ 2-1 (10 cm) | 30 | 8.4 | 247 | 28 | 10.1 | 0.25 | 1.1 | 0.5 | 56 | 33 | 59 | 8 | 55 | 23 | 1.2 | 3.6 |
| 28 | UJ 2-2 (50 cm) | 30 | 8.1 | 398 | 38 | 9.0 | 0.24 | 0.9 | 0.6 | 44 | 45 | 51 | 4 | 47 | 26 | 0.7 | 2.4 |
| 29 | UJ 2-3 (100 cm) | 22 | 8.4 | 597 | 33 | 9.7 | 0.23 | 0.9 | 0.5 | 58 | 54 | 42 | 4 | 73 | 31 | 0.6 | 2.9 |
| 30 | UJ 2-4 (130 cm) | 30 | 7.4 | 2150 | 3 | 4.7 | | 0.5 | 0.3 | 29 | 58 | 13 | 30 | 35 | | | |
| 31 | UJ 2 basalt 1 (bedrock) | | | | | | | | | | | | | | 81 | 0.4 | 5.8 |
| 32 | UJ 2-5 (180 cm) | 26 | 7.4 | 4260 | 28 | 7.0 | | 0.3 | 0.5 | 40 | 79 | 12 | 9 | 60 | | | |
| | Amrawah Colour Change | | | | | | | | | | | | | | | | |
| 33 | AM Fw 1 (150 cm) | 19 | 8.7 | 175 | 21 | 12.0 | 0.26 | 1.1 | 0.4 | | 61 | 36 | 3 | 4 | 26 | 1.6 | 5.0 |
| 34 | Am Fw 2 (250 cm) | 11 | 8.8 | 253 | 18 | 15.9 | | 0.7 | 0.7 | | 71 | 25 | 4 | n.a. | | | |
| 35 | Am Fw 3 (300 cm) | 26 | 9.2 | 155 | 36 | 9.1 | 0.24 | 0.5 | 0.5 | | 57 | 36 | 9 | 5 | 26 | 1.1 | 2.8 |
| | Amrawah Limestone/Basalt | | | | | | | | | | | | | | | | |
| 36 | Am 1 (100 cm) | 29 | 8.2 | 165 | 13 | 11.8 | 0.22 | 1.1 | 1.6 | 186 | 73 | 24 | 3 | 33 | 25 | 2.2 | 8.0 |
| 37 | Am 2 (160 cm) | 20 | 8.2 | 193 | 30 | 8.9 | 0.25 | 1.6 | 1.3 | | 71 | 20 | 8 | 76 | 26 | 1.5 | 2.3 |
| 38 | Am 3 (200 cm) | 18 | 8.3 | 175 | 29 | 9.4 | 0.24 | 1.2 | 0.9 | | 67 | 31 | 1 | 7 | 23 | 1.6 | 3.1 |
| 39 | Am Bw 1 (270 cm) | 30 | 8.5 | 163 | 23 | 10.9 | 0.16 | 1.4 | 0.9 | | 73 | 21 | 6 | 0 | 22 | 2.2 | 3.9 |
| 40 | Am Bw 2 (300cm) | 25 | 8.4 | 170 | 11 | 11.9 | 0.16 | 1.5 | 1.1 | | 75 | 23 | 2 | 0 | 23 | 2.2 | 7.4 |
| 41 | Am 4 (basalt bedrock) | | | | | | | | | | | | | | 68 | 1.3 | 10.6 |
| 42 | Am 5 (10 cm) | 13 | 7.9 | 211 | 0 | 16.0 | 0.25 | 3.1 | 2.3 | | 53 | 38 | 8 | 16 | 23 | 8.9 | 55.4 |
| 43 | Am 6 (60 cm) | 20 | 8.3 | 244 | 1 | 10.6 | 0.18 | 2.6 | 1.5 | | 64 | 30 | 7 | 37 | 22 | 3.4 | 41.9 |
| 44 | Am 7 (300 cm) | 20 | 8.5 | 180 | 38 | 7.1 | 0.20 | 0.7 | 0.6 | | 71 | 26 | 3 | 12 | 25 | 1.3 | 2.3 |
| 45 | AmO 20 (limestone bedrock) | | | | | | | | | | | | | | 12 | 0.3 | 0.1 |
| | Sandstone Ba'ja | | | | | | | | | | | | | | | | |
| 46 | Sandplateau 1 (10 cm) | 30 | 8.4 | 66 | 2 | 2.5 | 0.41 | 0.3 | 0.1 | 12 | 9 | 13 | 78 | 1 | 9 | 0.8 | 75.0 |
| 47 | Sandplateau 2 (30 cm) | 17 | 8.5 | 60 | 1 | 2.0 | 0.46 | 0.3 | 0.0 | 9 | 9 | 9 | 82 | 5 | 9 | 0.6 | 116.6 |
| 48 | Sandplateau 3 (50 cm) | 20 | 8.2 | 60 | 1 | 2.0 | 0.46 | 0.2 | 0.1 | 6 | 9 | 9 | 82 | 9 | 6 | 0.7 | 294.1 |
| 49 | Sandplateau 4 (70 cm) | 13 | 8.2 | 40 | 0 | 1.7 | 0.42 | 0.2 | 0.1 | 7 | 10 | 8 | 82 | 0 | 8 | 0.6 | 973.5 |
| 50 | Sandstone (bedrock) | | 8.5 | 52 | | 0.1 | 0.20 | | | | 4 | 7 | 89 | | 7 | 0.3 | 1383.5 |

(location no. 9 in Fig. 1), which could have provided local dust emissions. There is a strong similarity in clay mineralogy between the RMS on limestone, basalt, and the sandstone Lithosol. Except for the silicified limestone near Irbid, all clay minerals in the soils show some differences to the underlying bedrocks. Quartz is present in all samples.

In the Yarmouk Limestone profile, samples AB 1 and AB 2 are identical and show slightly higher crystallinity in minerals of the smectite group (height-to-width ratio of the peak) than the other soil samples. Samples AB 4–7 are characterised by higher illite contents in the deeper part in contrast to the upper part of the profile. Vermiculite amounts do not change with depth. In the limestone sample AB 8, which is composed of the clay mineral residues of the soft limestone, some palygorskite occurs, whereas illite is underrepresented, and vermiculite and chlorite are absent. The comparison with the nearby rock sample Yar 5 (characterised by less smectite, a lack of palygorskite, but the presence of some chlorite) illustrates the local variations of the clay mineral assemblages in the rocks. As smectite normally forms out of vermiculite, and vermiculite out of illite, a direct relation between the limestone and the superimposed RMS cannot be verified, although parts of the smectite could be inherited from the limestone bedrock.

Strikingly, virtually no change in the clay mineral composition occurs in samples AB 7 to AB 4. Across the 150 cm depth of the profile, neither clay weathering nor clay mineral neo-formation is indicated. Only the transition to the upper part of the profile, with decreasing illite and increasing smectite content, might be interpreted as an effect of pedogenesis. Possible explanations for this are that the lower part of the soil profile on limestone developed either (a) in one or few depositional events or (b) over a longer period of time under constant environmental conditions. Another explanation could be homogeneous clay neoformation due to isovolumetric replacement. In this case, the decreasing amounts of oxalate-extractable aluminium (Table 2) towards the top of the profile could reflect increasing crystallisation of amorphous clay minerals.

In comparison, the caliche AB 10 has palygorskite and little kaolinite. The Wadi Shellalah Chalk, in contrast, contains high levels of montmorillonite and palygorskite, as well as illite. Since kaolinite is lacking, the

Please cite this article as: Lucke, B., et al., Red Mediterranean Soils in Jordan: New insights in their origin, genesis, and role as environmental archives, Catena (2013), http://dx.doi.org/10.1016/j.catena.2013.04.006

**Table 3**
Chemical analyses: major elements. The bedrock samples were marked with colour: orange for the calcareous rocks, grey for basalt, yellow for sandstone, and light red for weathering crusts of the rocks. For the bedrock samples AB 8, AB 10 and I 0 results were recalculated by subtracting the mass contents of $CaCO_3$ as determined in Table 2, assuming that the results refer only to the $CaCO_3$-free residue.

| % | $Al_2O_3$ | $SiO_2$ | $Na_2O$ | MgO | $K_2O$ | CaO | $TiO_2$ | MnO | $Fe_2O_3$ | $P_2O_5$ | LOI[a] | SUM |
|---|---|---|---|---|---|---|---|---|---|---|---|---|
| Yarmouk Limestone | | | | | | | | | | | | |
| AB 1 (50 cm) | 8.3 | 28.7 | 0.1 | 1.6 | 0.6 | 26.0 | 0.7 | 0.1 | 4.6 | 0.4 | 29.1 | 100.3 |
| AB 2 (100 cm) | 7.8 | 27.4 | 0.1 | 1.5 | 0.5 | 27.7 | 0.7 | 0.1 | 4.4 | 0.3 | 29.9 | 100.6 |
| AB 3 (150 cm) | 10.2 | 34.6 | 0.2 | 1.7 | 0.8 | 20.9 | 0.9 | 0.1 | 5.5 | 0.3 | 25.8 | 101.0 |
| AB 4 (200 cm) | 10.5 | 35.8 | 0.2 | 1.8 | 0.8 | 19.1 | 1.0 | 0.1 | 5.8 | 0.3 | 24.6 | 99.9 |
| AB 5 (250 cm) | 12.3 | 41.3 | 0.2 | 2.1 | 1.0 | 13.7 | 1.1 | 0.1 | 6.9 | 0.3 | 21.4 | 100.5 |
| AB 6 (300 cm) | 13.7 | 45.5 | 0.3 | 2.3 | 1.1 | 9.3 | 1.2 | 0.1 | 7.6 | 0.4 | 18.7 | 100.2 |
| AB 7 (350 cm) | 14.3 | 48.5 | 0.4 | 2.4 | 1.3 | 10.0 | 1.3 | 0.14 | 7.9 | 0.5 | 12.5 | 99.1 |
| AB 8 (bedrock) | 1.5 | 5.0 | 0.01 | 0.6 | 0.1 | 50.2 | 0.1 | 0.01 | 0.9 | 0.8 | 40.5 | 99.8 |
| AB 8 (residue without $CaCO_3$) | 14.6 | 50.0 | 0.1 | 5.6 | 1.2 | n.a. | 0.6 | 0.1 | 9.1 | 8.4 | n.a. | n.a. |
| Yarmouk C aliche | | | | | | | | | | | | |
| AB 9 (10 cm) | 13.7 | 51.5 | 0.2 | 1.5 | 0.8 | 5.7 | 1.4 | 0.2 | 7.6 | 0.2 | 17.2 | 99.8 |
| AB 10 (bedrock) | 0.9 | 4.3 | 0.01 | 0.6 | 0.1 | 51.5 | 0.1 | 0.02 | 0.6 | 0.4 | 41.3 | 99.8 |
| AB 10 (residue without $CaCO_3$) | 10.8 | 53.8 | 0.1 | 7.5 | 0.9 | n.a. | 1.0 | 0.2 | 7.9 | 4.7 | n.a. | n.a. |
| Irbid Silicified L imestone | | | | | | | | | | | | |
| I 14a (60 cm) | 13.1 | 57.9 | 0.2 | 1.1 | 0.6 | 2.8 | 1.6 | 0.2 | 7.3 | 0.1 | 14.1 | 98.9 |
| I 9 (200 cm) | 13.1 | 53.5 | 0.3 | 1.3 | 0.6 | 6.8 | 1.5 | 0.2 | 7.3 | 0.2 | 15.3 | 99.8 |
| I 4 (290 cm) | 6.5 | 14.7 | 0.03 | 0.9 | 0.3 | 37.6 | 0.4 | 0.03 | 3.5 | 0.3 | 35.5 | 99.8 |
| I 0 (bedrock) | 0.7 | 93.2 | 0.01 | 0.1 | 0.04 | 2.6 | 0.03 | 0.01 | 0.5 | 0.1 | 3.2 | 100.3 |
| I 0 (residue without $CaCO_3$) | 0.7 | 98.1 | 0.01 | 0.1 | 0.04 | n.a. | 0.03 | 0.01 | 0.5 | 0.1 | n.a. | n.a. |
| Abila R uins Rendzina -Regosol | | | | | | | | | | | | |
| AB 4-1 (5 cm) | 3.3 | 12.4 | 0.1 | 0.9 | 0.4 | 42.4 | 0.3 | 0.05 | 1.9 | 0.7 | 37.8 | 100.2 |
| AB 4-2a (8 cm) | | | | | | | | | | | | |
| AB 4 -2b (19 cm) | 2.7 | 10.7 | 0.1 | 0.8 | 0.3 | 43.9 | 0.2 | 0.03 | 1.6 | 0.7 | 38.3 | 99.4 |
| AB 4-3 (28 cm) | 3.3 | 12.7 | 0.1 | 0.9 | 0.4 | 42.4 | 0.3 | 0.04 | 1.8 | 0.7 | 37.8 | 100.4 |
| AB 4-4 (limestone) | 0.004 | 2.2 | 0.01 | 0.6 | 0.02 | 52.8 | 0.03 | 0.003 | 0.25 | 0.2 | 43.8 | 99.9 |
| Wadi el-Arab Lithosol | | | | | | | | | | | | |
| TZ 65 (10 cm) | 3.4 | 24.7 | 0.1 | 1.5 | 0.3 | 32.1 | 0.3 | 0.1 | 2.5 | 0.6 | 34.6 | 100.1 |
| TZ 66 (bedrock) | 1.0 | 2.7 | 0.01 | 0.6 | 0.1 | 51.9 | 0.1 | 0.01 | 0.6 | 0.1 | 42.9 | 100.2 |
| Umm Queis Basalt | | | | | | | | | | | | |
| UQ 9 (10 cm) | 13.0 | 43.2 | 0.2 | 2.6 | 0.8 | 10.0 | 1.2 | 0.1 | 7.4 | 0.3 | 20.6 | 99.4 |
| UQ 21 (160 cm) | 13.3 | 44.3 | 0.3 | 2.7 | 0.9 | 9.6 | 1.2 | 0.1 | 7.6 | 0.2 | 18.9 | 99.1 |
| UQ 23 (caliche) | 0.4 | 1.1 | 0.01 | 0.5 | 0.04 | 53.9 | 0.03 | 0.01 | 0.3 | 0.9 | 42.4 | 99.7 |
| Basalt UQ (bedrock) | 15.5 | 44.6 | 2.9 | 5.0 | 0.7 | 12.3 | 2.0 | 0.2 | 11.9 | 0.4 | 3.8 | 99.3 |
| Umm el-Jimal Basalt | | | | | | | | | | | | |
| UJ 2-1 (10 cm) | 9.2 | 41.0 | 0.5 | 3.1 | 1.4 | 17.1 | 1.0 | 0.2 | 5.7 | 0.2 | 20.3 | 99.9 |
| UJ 2-2 (50 cm) | 8.6 | 33.7 | 0.4 | 3.2 | 0.9 | 22.1 | 0.9 | 0.1 | 5.3 | 0.1 | 25.0 | 100.4 |
| UJ 2-3 (100 cm) | 9.6 | 35.1 | 0.5 | 3.5 | 0.8 | 19.8 | 1.0 | 0.1 | 5.9 | 0.1 | 24.0 | 100.4 |
| UJ 2-4 (130 cm) | | | | | | | | | | | | |
| UJ 2 basalt 1 (bedrock) | 14.8 | 40.8 | 2.3 | 6.3 | 0.5 | 13.8 | 2.3 | 0.2 | 12.9 | 0.4 | 6.0 | 100.2 |
| UJ 2-5 (180 cm) | | | | | | | | | | | | |
| Amrawah Colour Change | | | | | | | | | | | | |
| AM Fw 1 (150 cm) | 11.9 | 42.9 | 0.3 | 2.2 | 1.4 | 13.3 | 1.1 | 0.1 | 6.6 | 0.3 | 19.4 | 99.5 |
| Am Fw 3 (300 cm) | 9.5 | 37.0 | 0.3 | 1.8 | 1.2 | 20.3 | 0.9 | 0.1 | 5.4 | 0.4 | 23.0 | 99.9 |

[a]Loss of ignition.

(*continued on next page*)

**Table 3** (*continued*)

| % | $Al_2O_3$ | $SiO_2$ | $Na_2O$ | MgO | $K_2O$ | CaO | $TiO_2$ | MnO | $Fe_2O_3$ | $P_2O_5$ | LOI[a] | SUM |
|---|---|---|---|---|---|---|---|---|---|---|---|---|
| Amrawah Limestone/Basalt | | | | | | | | | | | | |
| Am 1 (100 cm) | 13.7 | 50.1 | 0.3 | 2.5 | 1.7 | 9.6 | 1.2 | 0.2 | 7.5 | 0.3 | 12.5 | 99.7 |
| Am 2 (160 cm) | 9.3 | 35.4 | 0.2 | 1.8 | 1.2 | 23.4 | 0.8 | 0.1 | 5.1 | 0.3 | 22.6 | 100.2 |
| Am 3 (200 cm) | 10.2 | 40.8 | 0.3 | 1.7 | 1.3 | 19.4 | 1.0 | 0.1 | 5.6 | 0.2 | 19.6 | 100.1 |
| Am Bw 1 (270 cm) | 12.2 | 38.0 | 0.3 | 2.0 | 1.6 | 16.5 | 1.3 | 0.1 | 9.6 | 0.3 | 17.8 | 99.7 |
| Am Bw 2 (300cm) | 14.1 | 44.3 | 0.4 | 2.3 | 1.7 | 10.1 | 1.5 | 0.1 | 10.5 | 0.3 | 14.4 | 99.7 |
| Am 4 (basalt bedrock) | 14.3 | 42.7 | 2.2 | 9.7 | 0.9 | 8.1 | 2.2 | 0.2 | 14.0 | 0.4 | 3.9 | 98.8 |
| Am 5 (10 cm) | 16.7 | 58.3 | 0.1 | 1.6 | 1.1 | 1.6 | 1.6 | 0.1 | 9.2 | 0.5 | 8.8 | 99.5 |
| Am 6 (60 cm) | 14.9 | 60.4 | 0.3 | 2.5 | 1.7 | 2.1 | 1.4 | 0.1 | 8.3 | 0.5 | 7.4 | 99.7 |
| Am 7 (300 cm) | 9.1 | 35.9 | 0.2 | 1.7 | 1.1 | 23.5 | 0.8 | 0.1 | 5.0 | 0.4 | 22.6 | 100.3 |
| AmO 20 (limestone bedrock) | 1.2 | 3.8 | 0.02 | 0.7 | 0.1 | 51.2 | 0.1 | 0.02 | 0.8 | 0.3 | 41.8 | 100.0 |
| Sandstone Ba'ja | | | | | | | | | | | | |
| Sandplateau 1 (10 cm) | 3.4 | 89.3 | 0.1 | 0.4 | 0.3 | 1.3 | 0.3 | 0.02 | 0.9 | 0.1 | 3.3 | 99.1 |
| Sandplateau 2 (30 cm) | 2.9 | 91.4 | 0.02 | 0.2 | 0.2 | 0.8 | 0.2 | 0.01 | 0.6 | 0.04 | 2.5 | 98.9 |
| Sandplateau 3 (50 cm) | 2.9 | 92.9 | 0.02 | 0.2 | 0.2 | 0.3 | 0.2 | 0.01 | 0.6 | 0.04 | 2.0 | 99.4 |
| Sandplateau 4 (70 cm) | 3.2 | 93.1 | 0.01 | 0.2 | 0.1 | 0.1 | 0.2 | 0.01 | 0.6 | 0.03 | 1.9 | 99.4 |
| Sandstone (bedrock) | 3.7 | 92.9 | 0.01 | 0.02 | 0.03 | 0.1 | 0.1 | 0.003 | 0.1 | 0.1 | 1.6 | 98.5 |

chalk hardly represents the sole allochthonous parent material of the RMS. However, it could have provided montmorillonite — while it is likely that palygorskite would have quickly become instable. In this context, the only soil that contains palygorskite in significant amounts is sample AB 7, which is close to the bedrock, and the Rendzina–Regosol of the ruins soil at Abila. Again, this confirms the immaturity of this soil and is an example for what can be provided from limestone bedrock residue.

In the RMS on silicified limestone near Irbid, the fully developed RMS in the upper part shows little change compared to the lower part, which was interpreted as partially weathered silicified limestone (samples I 4–I 0). Overall, vermiculite contents are low and only the amount of smectite varies slightly. At this location, inheritance from the limestone residue could be indicated due to the presence of vermiculite in the bedrock residue. Apart from the reduced amounts of vermiculite, the clay mineral assemblage of the Irbid profile is however very similar to the profile on Yarmouk Limestone. Aeolian additions might thus be present, but cannot be separated from the bedrock residue.

The colour-based identification of soil movement processes in the upper part of the Amrawah profile can to some degree be supported by the clay mineralogy, although most samples are very similar. In the case where a colour change can be observed without a corresponding basalt flow (profile "Amrawah Colour Change"), samples from both horizons are virtually identical. In the RMS separated by the basalt flow however (profile "Amrawah Limestone/Basalt"), some differences are discernible. There is significantly more illite in the paleosol under the basalt flow, while the amount of vermiculite increases in the RMS above the basalt flow. Muscovite is present in the paleosol, while hydrobiotite is present in the upper RMS but not below the basalt. Since muscovite/mica weather to vermiculite via hydrobiotite, and illite to vermiculite, the clay minerals of the upper RMS seem more strongly weathered and could have formed out of the clay mineral composition of the lower RMS. In fact, this might also have taken place at the location characterised by a colour change without separating basalt flow.

Regarding the possible contribution of the bedrock at the Amrawah profile, the smectite contents could be the result of illite and vermiculite weathering provided by the limestone. Kaolinite is not present, while the presence of feldspars may point to primary interlayers within the bedrocks, either of lithic sandstone or volcanogenic rock lenses or horizons. Compared to the RMS of the Yarmouk Limestone and the Irbid Silicified Limestone, the Amrawah profile shows very similar clay mineral assemblages, although apparently stronger weathering features are present near Yarmouk and Irbid. This is consistent with the aforementioned results.

A high similarity is demonstrated between the clay mineral assemblages of the RMS on basalt and that of the limestone RMS. These samples all show low or only trace amounts of illite, but very high amounts of smectite, vermiculite, and kaolinite. The larger amount of vermiculite could be explained by a more intensive clay mineral neo-formation in the basalt soil. However, the samples of UQ 13 and AB 3 superimpose each other completely, pointing to strong similarities between the clays of the RMS on basalt and the Yarmouk Limestone, which might be explained by Cretaceous volcanic material in the limestone (Lucke et al., 2012). One should note that Palygorskite could only be found in the immediate surface of the basalt soil although it is present in the bedrock. Therefore it may be taken as a marker for local chalk dust emissions, which is consistent with the clay mineral assemblage of the Abila ruins Rendzina–Regosol and the interpretation of $CaCO_3$-contents in the basalt RMS.

Finally, all samples from the sandstone Lithosol near Ba'ja show their own specific clay mineral association: high amounts of kaolinite, but only minor amounts of smectite, vermiculite and illite. There is no observable relation between profile depth and 2:1-layer mineral content in these samples. The sandstone parent rock, however, exclusively contains kaolinite. As smectite and vermiculite cannot be derived from the

Please cite this article as: Lucke, B., et al., Red Mediterranean Soils in Jordan: New insights in their origin, genesis, and role as environmental archives, Catena (2013), http://dx.doi.org/10.1016/j.catena.2013.04.006

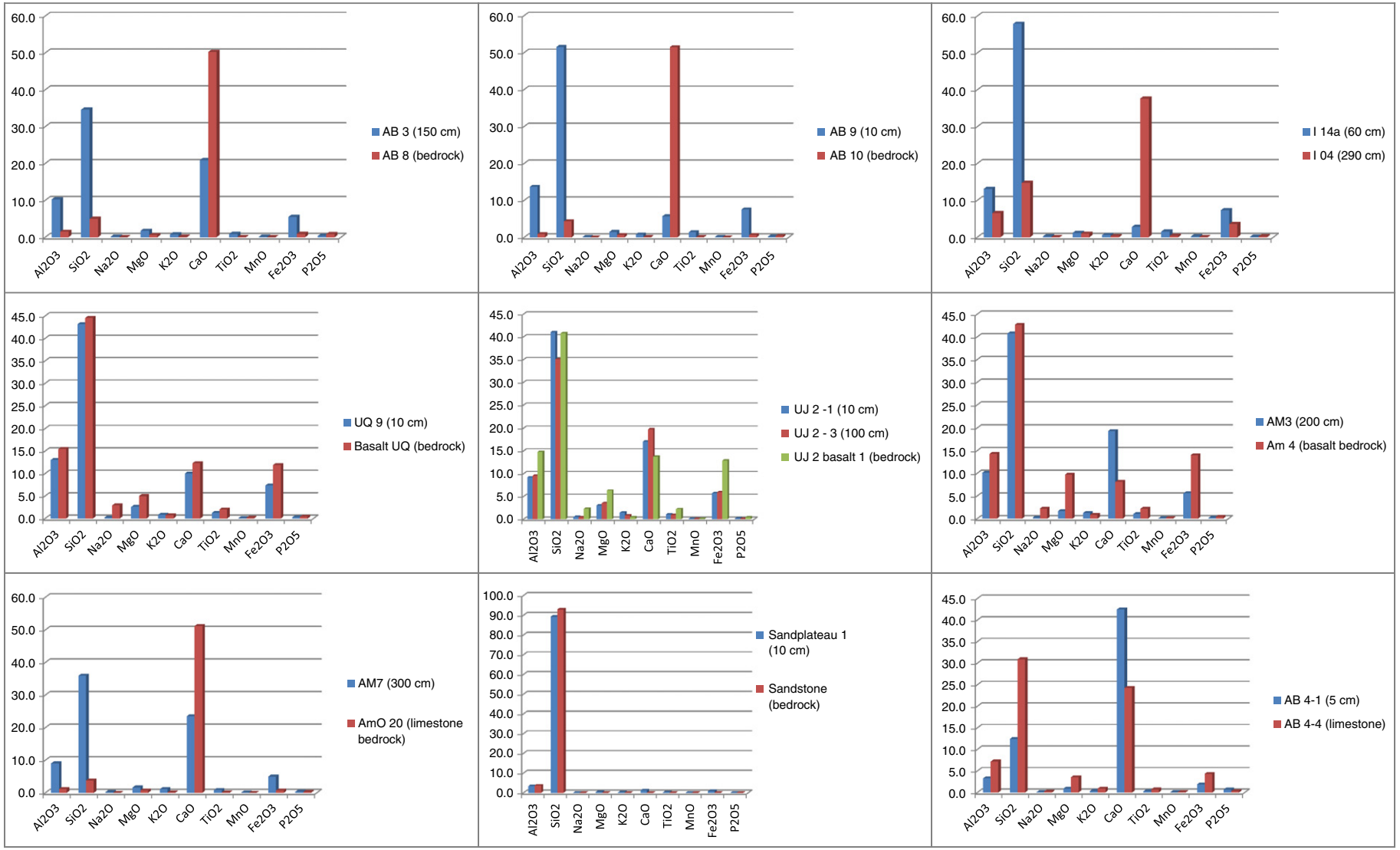


**Fig. 14.** Comparison of main elements in the topsoils and bedrocks of the investigated profiles.

Please cite this article as: Lucke, B., et al., Red Mediterranean Soils in Jordan: New insights in their origin, genesis, and role as environmental archives, Catena (2013), http://dx.doi.org/10.1016/j.catena.2013.04.006

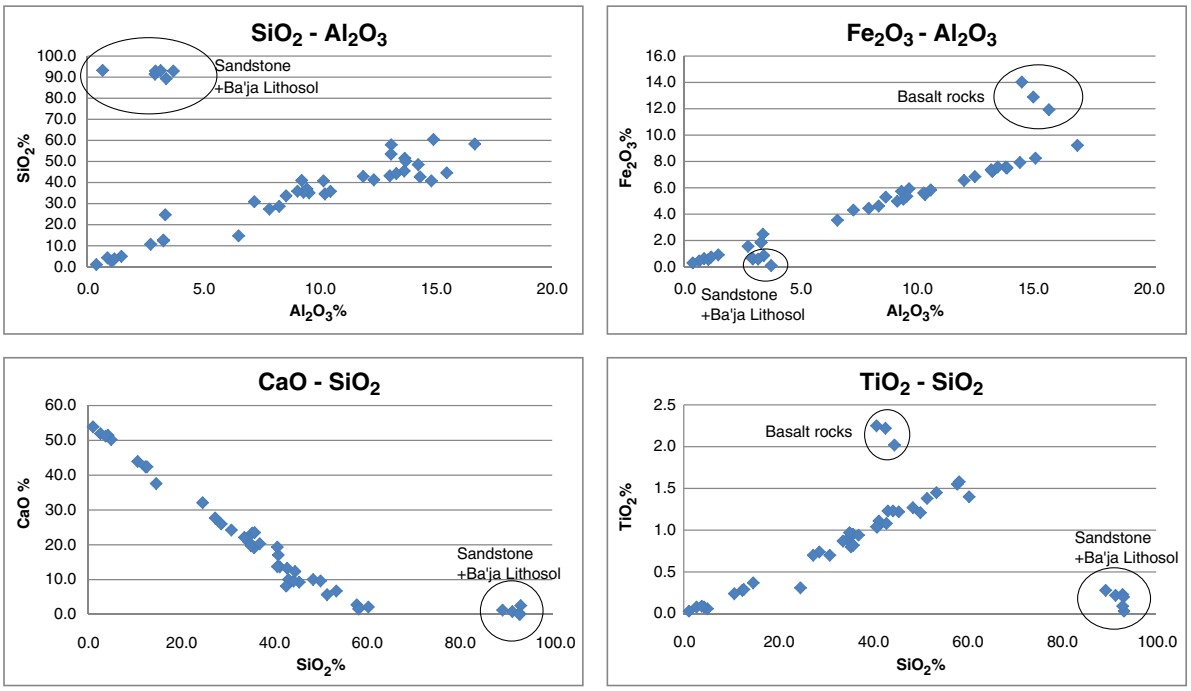


**Fig. 15.** Correlations of $SiO_2$, $Al_2O_3$, $Fe_2O_3$, $TiO_2$ and CaO in the investigated soils and bedrocks.

1:1-layer mineral kaolinite (at least under soil-forming conditions), the 2:1-layer minerals in the soil above the sandstone must originate from an external source: they probably are deposited aerosols.

## 5. Discussion

Although bedrock residue must have contributed to RMS formation in the investigation region, its importance seems to be limited, in particular for the RMS on limestone. For the RMS on basalt near Umm Queis, a genesis out of bedrock dissolution was assumed since the medium to coarse sand fraction (>250 to ≥1000 μm) of this soil still contains components of the source-rock paragenesis. This was confirmed by EDS microanalyses (Lucke, 2008). Calcium-rich feldspars of andesine to labradorite composition, augite-pyroxene, and magnetite could be identified as the primary components of the basaltic source rock. This soil genetic interpretation is supported by the corresponding regional distribution of soil properties with the bedrock (Schmidt et al., 2006) and studies of other RMS on basalt in Jordan (Moormann, 1959). In general, the pattern of soil distribution in Jordan points to an important role of local factors in their formation, as the deepest soils are located in the east, where wadis are least incised and drainage is minimal. Instead, soil variations are strongest in RMS on limestone on the deeply incised Mediterranean plateau, the level appearance of which seems to be the outcome of considerable soil movement (Khresat and Taimeh, 1988; Lucke, 2008; Schmidt et al., 2006; Taimeh, 1984). The National Soil Map and Land Use Project concluded that soil distribution in the country reflects the climate, since there is a correlation between clay and calcium carbonate contents and rainfall, and that an aeolian contribution to soil development is evident due to high silt fractions, especially in the east (NSM&LUP, 1993).

In a first field hypothesis on the degree to which bedrock could have contributed to the formation of RMS on limestone, it was assumed that varying hardness and $CaCO_3$-content of the soils might be connected with varying soil depth, or at least the karst structure of the bedrock (Lucke, 2008). However, for the RMS development on limestone, additional processes have to be considered. This is underlined by the RMS on silicified limestone near Irbid, which should to a large percentage consist of chert gravel if it had formed mainly by limestone dissolution, which is not the case. Only a small area of chert concentration exists, which is interpreted as the contact zone between weathering rock and fully developed RMS soil. Moreover, the largely identical composition of RMS on limestone and basalt in our study indicates that a large part of the parent material originates from an external source, although it does not dominate soil development on a regional scale.

Dust as a major source of RMS development has been widely discussed. According to Israelevich et al. (2006), there is a permanent reservoir of dust in the atmosphere over northern Africa, ready to be transported as soon as the appropriate synoptic conditions arise — even if no primary dust mobilisation occurs. To significantly support soil formation, however, even high dust deposition rates require the co-existence of rainfall. Additionally, the rates are highly variable in space and time. For example, 30% of the annual mineral dust deposition in 1992 occurred during only two dust storms in May (Kubilay et al., 2000). In this context, Jahn (1995) estimated that only a small fraction of the total solum of soils on the Golan Heights was derived from aerosols.

Saharan dust currently deposited in Israel contains $SiO_2$, Fe, Al, and to a lesser degree Na and K (Singer et al., 1992; Yaalon and Ganor, 1979. The dust which is transported from the Sahara to northern Israel consists mostly of clay minerals. Smectite and to a lesser degree kaolinite serve as marker for its Saharan provenance (Molinaroli, 1996). The clay-mineral free fraction is composed of 35–45% quartz, 30–40% calcite, 10–20% dolomite, 5–10% feldspar, 2% halite, and less than 1% gypsum (Singer et al., 1992). Possible dust sources in Sudan and Egypt are known to contain relatively large amounts of zircon and rutile, which are very weathering resistant minerals and should be enriched over time (Sindowski, 1956; Eltayeb et al., 2001, 256). This, in turn, could explain enrichment of zirconium and titanium in soils affected by deposition of aerosols from this source.

According to Yaalon and Ganor (1979) and Molinaroli (1996), the desert dust transported to Israel and Jordan originates from alluvial deposits in mountain valleys of the Sahara (mainly Egypt and Sudan), Sinai, and Negev, ultimately coming from old lake beds and weathered minerals from the mountains. In Israel, the total dust fall is composed of a uniform local background with superimposed pulses of desert dust storms (Ganor and Foner, 1996). However,

Please cite this article as: Lucke, B., et al., Red Mediterranean Soils in Jordan: New insights in their origin, genesis, and role as environmental archives, Catena (2013), http://dx.doi.org/10.1016/j.catena.2013.04.006

**Table 4**
Chemical analyses: minor elements. The bedrock samples were marked with colour: orange for the calcareous rocks, grey for basalt, yellow for sandstone, and light red for weathering crusts of the rocks. For the bedrock samples AB 8, AB 10 and I 0 results were recalculated by subtracting the mass contents of $CaCO_3$ as determined in Table 2, assuming that the results refer only to the $CaCO_3$-free residue.

| [ppm] | V | Cr | Co | Ni | Cu | Zn | Ga | (As) | Rb | Sr | Y | Zr | Nb | Mo | Ba | Hf | Ta | W | (Pb) | Bi | La | Ce | Th | U |
|---|---|---|---|---|---|---|---|---|---|---|---|---|---|---|---|---|---|---|---|---|---|---|---|---|
| Yarmouk Limestone | | | | | | | | | | | | | | | | | | | | | | | | |
| AB 1 (50 cm) | 104 | 73 | 19 | 41 | 15 | 101 | 14 | 2 | 36 | 239 | 28 | 149 | 17 | <1 | 394 | 2 | <1 | <1 | 12 | <1 | 25 | 75 | 8 | 5 |
| AB 2 (100 cm) | 98 | 99 | 19 | 45 | 12 | 108 | 13 | 3 | 33 | 246 | 29 | 145 | 16 | <1 | 398 | 2 | <1 | <1 | 8 | 2 | 25 | 31 | 7 | <1 |
| AB 3 (150 cm) | 130 | 124 | 22 | 54 | 10 | 118 | 16 | 5 | 42 | 216 | 34 | 186 | 19 | <1 | 467 | 3 | <1 | <1 | 9 | 2 | 24 | 50 | 11 | 5 |
| AB 4 (200 cm) | 124 | 96 | 21 | 52 | 18 | 116 | 16 | 2 | 42 | 209 | 34 | 191 | 19 | <1 | 433 | 4 | <1 | <1 | 13 | 1 | 39 | 83 | 16 | 2 |
| AB 5 (250 cm) | 150 | 139 | 26 | 66 | 15 | 123 | 18 | 4 | 50 | 191 | 40 | 216 | 22 | <1 | 489 | 5 | <1 | 3 | 15 | <1 | 38 | 84 | 14 | 5 |
| AB 6 (300 cm) | 161 | 159 | 28 | 82 | 38 | 129 | 18 | 7 | 56 | 181 | 41 | 228 | 24 | <1 | 517 | 7 | <1 | 5 | 15 | 2 | 44 | 83 | 14 | 3 |
| AB 7 (350 cm) | 161 | 164 | 28 | 98 | 43 | 199 | 19 | 9 | 61 | 202 | 47 | 251 | 25 | <1 | 434 | 5 | <1 | 3 | 13 | <1 | 45 | 82 | 10 | 5 |
| AB 8 (bedrock) | 50 | 58 | 6 | 67 | 9 | 199 | 3 | 5 | 3 | 484 | 28 | 34 | 2 | 9 | 27 | <1 | 2 | <1 | <1 | 2 | 20 | 11 | 3 | 12 |
| AB 8 (residue without $CaCO_3$) | 500 | 580 | 60 | 670 | 90 | 1990 | 30 | 50 | 30 | 4840 | 280 | 340 | 20 | 90 | 270 | n.a. | 20 | n.a. | n.a. | 20 | 200 | 110 | 30 | 120 |
| Yarmouk Caliche | | | | | | | | | | | | | | | | | | | | | | | | |
| AB 9 (10 cm) | 147 | 124 | 28 | 72 | 33 | 108 | 19 | 8 | 56 | 115 | 44 | 320 | 26 | 3 | 484 | 9 | 2 | 4 | 19 | 2 | 38 | 131 | 20 | 5 |
| AB 10 (bedrock) | 14 | 26 | 3 | 5 | 2 | 51 | 5 | 2 | 1 | 408 | 22 | 35 | 3 | 10 | 91 | <1 | <1 | <1 | <1 | 2 | 12 | 31 | 4 | 8 |
| AB 10 (residue without $CaCO_3$) | 175 | 325 | 37.5 | 62.5 | 25 | 638 | 62.5 | 25 | 12.5 | 5100 | 275 | 438 | 37.5 | 125 | 1138 | n.a. | n.a. | n.a. | n.a. | 25 | 150 | 388 | 50 | 100 |
| Irbid Silicified Limestone | | | | | | | | | | | | | | | | | | | | | | | | |
| I 14a (60 cm) | 161 | 123 | 38 | 69 | 52 | 105 | 18 | 4 | 46 | 120 | 43 | 404 | 30 | 2 | 414 | 10 | <1 | 5 | 22 | 2 | 35 | 171 | 22 | 3 |
| I 9 (200 cm) | 164 | 145 | 38 | 63 | 32 | 116 | 18 | 4 | 45 | 135 | 42 | 325 | 29 | <1 | 432 | 8 | <1 | 3 | 19 | 1 | 31 | 98 | 25 | 6 |
| I 4 (290 cm) | 81 | 31 | 10 | 16 | 5 | 76 | 12 | 3 | 23 | 116 | 14 | 56 | 10 | <1 | 86 | 1 | <1 | <1 | 4 | 1 | 13 | 44 | 6 | 5 |
| I 0 (bedrock) | 12 | 12 | 1 | 8 | <1 | 14 | 4 | <1 | <1 | 39 | 7 | 11 | 3 | 5 | 494 | <1 | <1 | <1 | 7 | 10 | <1 | 7 | 5 | 2 |
| I 0 (residue without $CaCO_3$) | 12.6 | 12.6 | 1.05 | 8.42 | n.a. | 14.7 | 4.21 | n.a. | n.a. | 41.1 | 7.37 | 11.6 | 3.16 | 5.26 | 520 | n.a. | n.a. | n.a. | 7.37 | 10.5 | n.a. | 7.37 | 5.26 | 2.11 |
| Abila Ruins Rendzina-Regosol | | | | | | | | | | | | | | | | | | | | | | | | |
| AB 4-1 (5 cm) | 52 | 77 | 10 | 22 | 10 | 107 | 8 | <1 | 21 | 364 | 20 | 69 | 7 | 2 | 254 | <1 | <1 | <1 | 19 | 2 | <1 | 17 | 4 | 4 |
| AB 4-2a (8 cm) | | | | | | | | | | | | | | | | | | | | | | | | |
| AB 4 -2b (19 cm) | 51 | 43 | 8 | 20 | 8 | 105 | 4 | <1 | 15 | 383 | 19 | 57 | 7 | <1 | 269 | <1 | <1 | <1 | 24 | 2 | 7 | 45 | 5 | 4 |
| AB 4-3 (28 cm) | 51 | 76 | 9 | 21 | 5 | 103 | 7 | <1 | 20 | 365 | 22 | 71 | 7 | <1 | 253 | <1 | 2 | <1 | 18 | 2 | 13 | 20 | 5 | 5 |
| AB 4-4 (limestone) | 5 | 25 | 1 | 1 | 1 | 24 | 3 | <1 | 1 | 270 | 2 | 7 | 2 | <1 | 1029 | <1 | <1 | <1 | 3 | 1 | 1 | 1 | 4 | <1 |
| Wadi el-Arab Lithosol | | | | | | | | | | | | | | | | | | | | | | | | |
| TZ 65 (10 cm) | 44 | 49 | 14 | 10 | 3 | 162 | 6 | <1 | 5 | 298 | 18 | 77 | 7 | <1 | 192 | <1 | 1 | <1 | 3 | 3 | 11 | 3 | 5 | <1 |
| TZ 66 (bedrock) | 24 | 10 | 5 | 3 | 2 | 157 | 2 | 2 | 3 | 249 | 7 | 27 | 3 | 10 | 84 | <1 | <1 | <1 | <1 | 3 | 6 | 21 | 5 | 5 |
| Umm Queis Basalt | | | | | | | | | | | | | | | | | | | | | | | | |
| UQ 9 (10 cm) | 141 | 112 | 28 | 60 | 19 | 102 | 18 | 5 | 50 | 174 | 35 | 222 | 25 | <1 | 522 | 6 | 1 | <1 | 26 | 1 | 31 | 96 | 16 | 5 |
| UQ 21 (160 cm) | 144 | 111 | 30 | 66 | 35 | 96 | 18 | 6 | 51 | 187 | 35 | 232 | 24 | <1 | 546 | 5 | <1 | 1 | 28 | <1 | 39 | 110 | 12 | 4 |
| UQ 23 (caliche) | 5 | 32 | 3 | <1 | 2 | 28 | 3 | <1 | <1 | 385 | 17 | 24 | 2 | 20 | 56 | <1 | <1 | <1 | <1 | 2 | 14 | 26 | 4 | 9 |
| Basalt UQ (bedrock) | 230 | 182 | 46 | 74 | 60 | 105 | 22 | 1 | 5 | 521 | 25 | 151 | 21 | 2 | 450 | 7 | <1 | 6 | 3 | <1 | 18 | 45 | 7 | <1 |
| Umm el-Jimal Basalt | | | | | | | | | | | | | | | | | | | | | | | | |
| UJ 2-1 (10 cm) | 142 | 86 | 29 | 57 | 11 | 81 | 15 | 3 | 42 | 265 | 33 | 273 | 18 | <1 | 329 | 6 | <2 | 2 | 14 | <2 | 25 | 100 | 10 | <3 |
| UJ 2-2 (50 cm) | 119 | 69 | 22 | 53 | 115 | 68 | 13 | 9 | 31 | 299 | 25 | 202 | 17 | <1 | 221 | 4 | <2 | <2 | 5 | <2 | 25 | 68 | 3 | 5 |
| UJ 2-3 (100 cm) | 139 | 80 | 28 | 61 | 28 | 64 | 16 | 7 | 29 | 348 | 26 | 185 | 17 | <1 | 207 | 5 | <2 | <2 | 5 | <2 | 21 | 62 | 7 | 5 |
| UJ 2 basalt 1 (bedrock) | 261 | 228 | 51 | 118 | 57 | 103 | 20 | 5 | 5 | 668 | 26 | 166 | 28 | <1 | 289 | 7 | <2 | 6 | <4 | <2 | 22 | 45 | 8 | 7 |
| Amrawah Colour Change | | | | | | | | | | | | | | | | | | | | | | | | |
| AM Fw 1 (150 cm) | 137 | 98 | 23 | 54 | 23 | 111 | 23 | 5 | 56 | 183 | 35 | 248 | 22 | <1 | 291 | 6 | <1 | <1 | 16 | <1 | 39 | 86 | 15 | 5 |
| Am Fw 3 (300 cm) | 119 | 75 | 21 | 42 | 28 | 101 | 28 | 4 | 45 | 187 | 32 | 219 | 18 | <1 | 207 | 3 | <1 | <1 | 9 | 1 | 34 | 64 | 11 | 4 |
| Amrawah Limestone/Basalt | | | | | | | | | | | | | | | | | | | | | | | | |
| Am 1 (100 cm) | 148 | 137 | 31 | 70 | 24 | 121 | 24 | 8 | 63 | 171 | 44 | 288 | 26 | <1 | 383 | 5 | 2 | 5 | 12 | 1 | 43 | 86 | 13 | 4 |
| Am 2 (160 cm) | 125 | 70 | 26 | 42 | 8 | 99 | 8 | 2 | 44 | 183 | 32 | 185 | 18 | <1 | 275 | 1 | <1 | <1 | 8 | <1 | 19 | 106 | 8 | <1 |
| Am 3 (200 cm) | 129 | 79 | 22 | 42 | 13 | 99 | 13 | 3 | 47 | 160 | 34 | 270 | 21 | <1 | 263 | 4 | <1 | <1 | 6 | 2 | 25 | 82 | 13 | 7 |
| Am Bw 1 (270 cm) | 136 | 144 | n.a. | 115 | n.a. | 153 | 22 | n.a. | 73 | 164 | 46 | 356 | 33 | n.a. | 358 | n.a. | n.a. | n.a. | 14 | n.a. | n.a. | n.a. | 11 | n.a. |
| Am Bw 2 (300 cm) | 175 | 173 | n.a. | 133 | n.a. | 164 | 22 | n.a. | 82 | 175 | 54 | 391 | 37 | n.a. | 385 | n.a. | n.a. | n.a. | 19 | n.a. | n.a. | n.a. | 12 | n.a. |
| Am 4 (basalt bedrock) | 235 | 423 | 69 | 308 | 73 | 125 | 73 | 4 | 9 | 471 | 32 | 197 | 27 | 3 | 628 | 6 | 2 | 6 | 2 | 1 | 22 | 54 | 8 | 4 |
| Am 5 (10 cm) | 140 | 146 | 27 | 142 | 85 | 128 | 85 | 4 | 24 | 121 | 55 | 412 | 30 | <1 | 1080 | 8 | 3 | 7 | 13 | <1 | 52 | 129 | 25 | 4 |
| Am 6 (60 cm) | 163 | 179 | 23 | 99 | 46 | 152 | 46 | 6 | 64 | 124 | 51 | 385 | 24 | <1 | 424 | 8 | 4 | 4 | 16 | <1 | 54 | 120 | 14 | 5 |
| Am 7 (300 cm) | 104 | 74 | 18 | 43 | 17 | 105 | 17 | 3 | 46 | 166 | 29 | 199 | 17 | <1 | 210 | 2 | <1 | <1 | 4 | 1 | 21 | 81 | 10 | 9 |
| AmO 20 (limestone bedrock) | 32 | 16 | 6 | 6 | 4 | 41 | 4 | 3 | 2 | 482 | 15 | 44 | 3 | 8 | 129 | <1 | <1 | <1 | <1 | 1 | 5 | 33 | 4 | 8 |
| Sandstone Ba´ja | | | | | | | | | | | | | | | | | | | | | | | | |
| Sandplateau 1 (10 cm) | 23 | 17 | 4 | 4 | <1 | 21 | 5 | <1 | 7 | 104 | 15 | 193 | 5 | 3 | 86 | <1 | <1 | <1 | 14 | 10 | 2 | 52 | 5 | 3 |
| Sandplateau 2 (30 cm) | 24 | 16 | 4 | <1 | <1 | 16 | 5 | <1 | 5 | 88 | 14 | 148 | 4 | 3 | 53 | <1 | <1 | <1 | 10 | 9 | <1 | 31 | 6 | 3 |
| Sandplateau 3 (50 cm) | 19 | 14 | 2 | <1 | <1 | 17 | 4 | <1 | 3 | 85 | 15 | 224 | 4 | 3 | 60 | <1 | <1 | <1 | 15 | 10 | <1 | 54 | 10 | 2 |
| Sandplateau 4 (70 cm) | 22 | 14 | 4 | <1 | <1 | 17 | 5 | <1 | 3 | 83 | 14 | 149 | 4 | 2 | 50 | <1 | <1 | <1 | 12 | 9 | <1 | 45 | 11 | 2 |
| Sandstone (bedrock) | 12 | 6 | <1 | <1 | <1 | 4 | 5 | <1 | <1 | 83 | 12 | 75 | 3 | 3 | 23 | <1 | <1 | <1 | 11 | 9 | 2 | 28 | 10 | <1 |

only 1 to 7% of the transported dust is deposited (Yaalon and Ganor, 1979). According to Ganor and Foner (1996), the clay mineral assemblages vary in relation to the origin of the storm trajectories. With respect to the Jordanian soils of our study, aerosols should mainly be transported with the prevailing western winds.

According to Ganor (1975), dust settling without rain has less than 20% clay, while pluvio-aeolian dust contains 50–60% clay. Increased clay mineral deposition connected with historic periods of higher precipitation might explain the clay-rich texture of red paleosols in Hamra–Kurkar sequences in the coastal plain of Israel (Issar and Bruins, 1983). While the composition of the Negev loess is similar to dust coming today from the deserts of northern Africa, Early Pleistocene sandy deposits are overlain by alternating layers of clay and silt. The uppermost loess blanket (50 cm of 11 m), presumably of Holocene age, however, has a low clay content of 25%. Therefore, Issar and Bruins (1983) concluded that the extent and character of aeolian deposition has changed since the end of the Ice Age. Dating of soils and paleowaters in the Negev indicated that depositional processes were active mainly from 100,000 to 10,000 BC (Issar et al., 1987). In this context, Nowell et al. (2003) dated Red Mediterranean Soils in Jordan according to

Please cite this article as: Lucke, B., et al., Red Mediterranean Soils in Jordan: New insights in their origin, genesis, and role as environmental archives, Catena (2013), http://dx.doi.org/10.1016/j.catena.2013.04.006

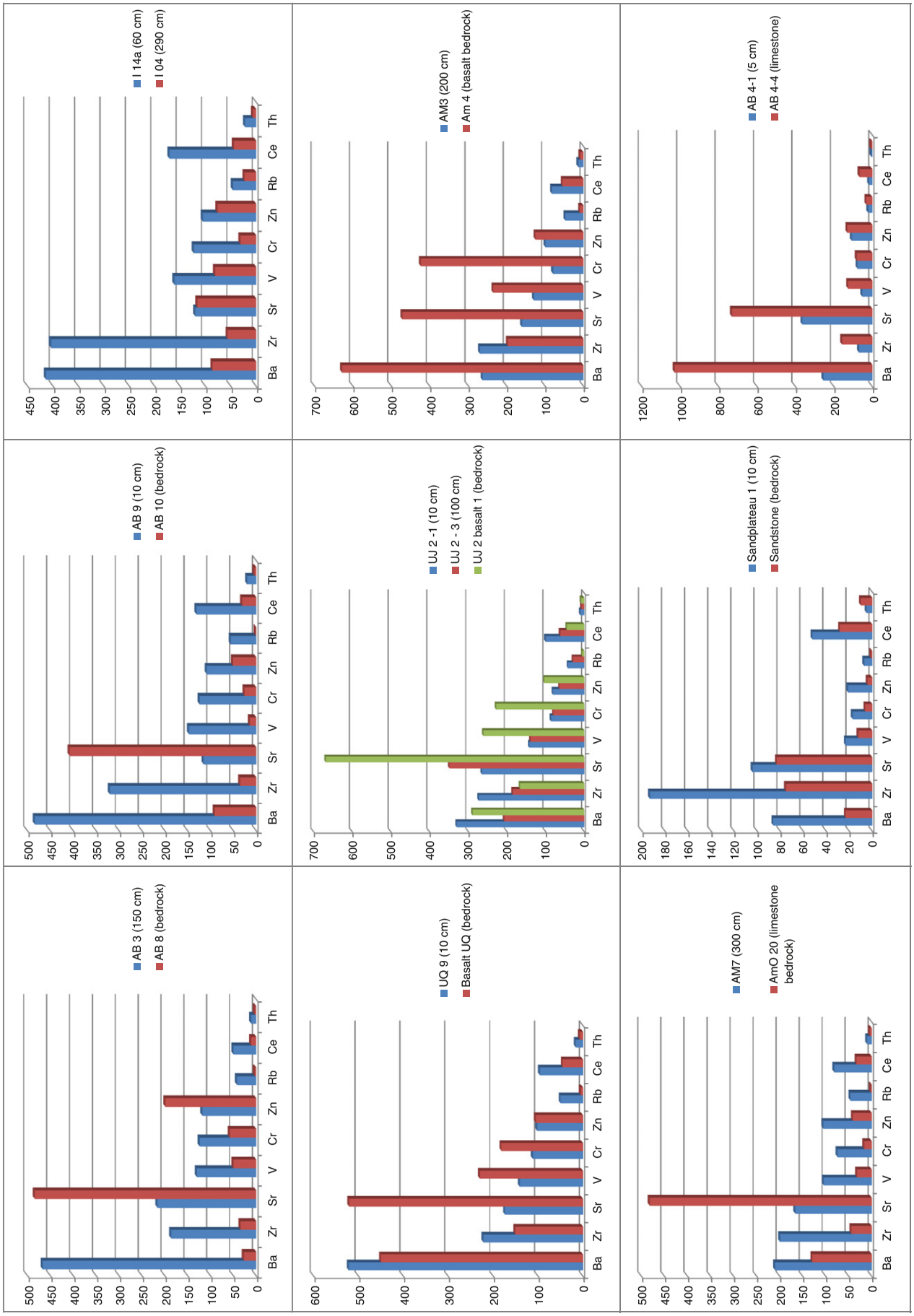


**Fig. 16.** Comparison of some rare elements in the topsoils and bedrocks of the investigated profiles.

**Table 5**
Clay mineralogy of examined soils. xxx represent major components, xx the presence of the mineral, and x traces. The bedrock samples were marked with colour: orange for the calcareous rocks, grey for basalt, yellow for sandstone, and light red for weathering crusts of the rocks.

| | Illite | Vermiculite | Montmorillonite (smectite) | Kaolinite | Chlorite | Palygorskite | Quartz | Muscovite (mica) | Hydrobiotite | Talc | Feldspars | Rutile | other |
|---|---|---|---|---|---|---|---|---|---|---|---|---|---|
| Yarmouk Limestone | x | xx | xxx | xxx | (x) | | xx | | | | | | |
| AB 1 (50 cm) | x | xx | xxx | xxx | | | xx | | | | | | |
| AB 2 (100 cm) | x | xx | xxx | xxx | | | xx | | | | | | |
| AB 3 (150 cm) | xx | xxx | xxx | xxx | x | | xx | | | | | | |
| AB 4 (200 cm) | xx | xx | xxx | xxx | x | | xx | | | | | | |
| AB 5 (250 cm) | xx | xx | xxx | xxx | x | | xx | | | | | | |
| AB 6 (300 cm) | xx | xx | xxx | xxx | x | | xx | | | | | | |
| AB 7 (350 cm) | x | | xxx | x | | xx | xx | | | | | | |
| AB 8 (bedrock) | x | | xxx | x | | xx | xx | | | | | | |
| Yarmouk Limestone II | | | | | | | | | | | | | |
| Yar1 Mitte (150 cm) | x | | xx | xx | | | xx | | | | | | |
| Yar1 Mitte unten (250 cm) | | x | xx | xx | | | xx | | | | | | |
| Yar 5 (bedrock) | x | | x | xx | xx | | xx | | | | | | |
| Yarmouk Caliche | | | | | | | | | | | | | |
| AB 10 (bedrock) | | | | x | | xx | xx | | | | | | |
| Abraded Chalk Exposure | | | | | | | | | | | | | |
| Wadi Shellalah chalk | x | | xxx | | | xxx | xx | | | | | | |
| Irbid Silicified Limestone | | | | | | | | | | | | | |
| I 15a (30 cm) | | | xx | xx | x | | xx | | | | | | |
| I 11a (150 cm) | | | xx | xx | | | xx | | | | | | |
| I 09 (215 cm) | x | x | xxx | xxx | | | xxx | | | | | | |
| I 08 (235 cm) | | | xx | xx | | | xx | | | | | | |
| I 04 (320 cm) | x | x | xxx | xxx | | | xxx | | | | | | |
| I 01 (380 cm) | x | | xx | xx | | | xx | | | | | | |
| I 00 (bedrock) | x | | x | | | | xx | | | | | | |
| Abila R uins Rendzina-Regosol | | | | | | | | | | | | | |
| AB 4-1 (5 cm) | x | xx | xx | xx | | xx | xx | | | | | | |
| AB4-2a (8 cm) | | x | xx | xx | | x | xx | | | | | | |
| AB 4-3 (28 cm) | | | xx | xx | | x | xx | | | | | | |
| AB 4-4 (limestone) | xx | x | x | | | xx | x | | | | xx | | |
| Umm Queis Basalt | | | | | | | | | | | | | |
| Basaltboden UQ (surface) | xx | xxx | xxx | xxx | xx | x | xx | | | x | x | x? | |
| UQ 11 (60 cm) | | x | xx | xx | | | xx | | | | | | |
| UQ 13 (100 cm) | x | xxx | xxx | xxx | | | xx | | | | | | |
| UQ 20 (160 cm) | | x | xx | xx | | | xx | | | | | | |
| UQ 23 (calcareous crust) | | | | x | xx | xx | xx | xx | x | | xx | | |
| Basalt UQ (bedrock) | | | | | | x | x | | | | xx | | x |
| Amrawah Colour Change | | | | | | | | | | | | | |
| AM Fw 1 (150 cm) | xxx | xx | xx | xxx | x | | xx | | | | | | |
| Am Fw 2 (250 cm) | xxx | xx | xx | xxx | x | | xx | | | | | | |
| Am Fw 3 (300 cm) | xxx | xx | xx | xxx | x | | xx | | | | | | |
| Amrawah Limestone/Basalt | | | | | | | | | | | | | |
| AmW 01 (10 cm) | | xx | xx | xx | xx | | xx | | xx | | | | |
| AmW 05 (170 cm) | x | xx | xx | xx | x | | xx | | xx | | | | |
| Am 4 (basalt bedrock) | | | | | | | | | | | | | |
| AmO 5 (45 cm) | xx | | xx | xx | | | xx | xx | | | | | |
| AmO 15 (255 cm) | x | x | xx | xx | xx | | xx | | | | | | |
| AmO 18 (335 cm) | x | | xx | xx | | | xx | | | | | | |
| AmO 20 (limestone bedrock) | xx | xx | x | | xx | xx | xx | | | | xx | | |
| Sandstone Ba'ja | | | | | | | | | | | | | |
| Sandplateau 1 (10 cm) | xx | xx | xx | xxx | | | xx | | | | | | |
| Sandplateau 4 (70 cm) | x | xx | xx | xxx | | | xx | | | | | | |
| Sandstone (bedrock) | | | | xxx | | | x | | | | | | |

x: traces, xx:present, xxx: abundant.

Mousterian artefacts at 125,000 years and older. As the oldest artefacts were mostly found deep in the profiles, they suggest a continuous role of long-range aeolian deposition for soil formation, even if it occurred at the low rates measured by Singer et al. (1992) and was limited to the period found by Issar and Bruins (1983).

The clear correlation between enrichment of $SiO_2$, $Al_2O_3$, and $Fe_2O_3$ in our study points to montmorillonite as main allochthonous addition. This agrees with Molinaroli (1996), who stated that smectite is a marker mineral for additions from the most likely dust source: Egypt and Sudan. According to Eltayeb et al. (2001, 254), dust from Sudan is characterised by a major increase of Ti and Zr in the fine particle fraction, which is to some degree also true for Rb. This matches our results, as it seems that these elements were strongly enriched during pedogenesis. To judge from the enrichment of elements and degree of soil development, the RMS on caliche near the village Yarmouk seems to be very old despite its shallowness. Possibly, this RMS is very shallow due to a limited contribution of bedrock dissolution.

Dissolution of limestone is not necessarily reflected by the geochemical composition of the soils. The Ti/Zr ratios of the sedimentary rocks vary, and the distribution of main elements suggests that the insoluble residue of the limestone consists largely of clay minerals with a similar composition as the aerosols. It seems possible therefore, that similar dust falls already occurred in the Cretaceous during formation of the calcareous rocks. Furthermore, it seems probable that Cretaceous and Holocene volcanic material, as for example documented from Syria

Please cite this article as: Lucke, B., et al., Red Mediterranean Soils in Jordan: New insights in their origin, genesis, and role as environmental archives, Catena (2013), http://dx.doi.org/10.1016/j.catena.2013.04.006

ARTICLE IN PRESS



(Krienitz et al., 2007), also contributed to soil development in some limestones.

Local dust emissions also seem to play a role for RMS development. This is indicated by $CaCO_3$-contents and palygorskite in the basalt soil. Eltayeb et al. (2001, 261) reported that Sudanian dust settling in Israel and Syria is strongly enriched with Ca, which points to local and regional emissions of this element. Further evidence for addition on a regional scale comes from K-bearing feldspars and granitoidic fragments of medium sand size in the RMS on basalt near Umm Queis, which must have been transported by heavy dust storms over distances of 400 km (Lucke, 2008, 130),

Earlier investigations of young, initial soils formed on limestone Regolith of historic ruins in Jordan found that these soils are barely weathered and consist mainly of microfossils, bone and pottery fragments, as well as calcite pieces (Lucke, 2008, 129). This is in agreement with the current study and indicates very limited soil development and deposition of aerosols during the past ~1000 years. The change of RMS development at Umm el Jimal indicates increasing aridity and a growing share of silt deposition at some point of time during the younger history of this RMS. It is likely that the end of RMS development at Umm el Jimal and increase of silt deposition coincided with deposition of the uppermost loess blanket in the Negev, which Issar and Bruins (1983) dated to the Holocene. Since no in-situ rubefication of soils in Jordan could so far be dated to periods later than the Neolithic (Lucke, 2008), it seems likely that the investigated RMS formed mainly during the Pleistocene.

Last but not the least, the presence of a 'bleached zone' at the rock–soil transition of the RMS on Yarmouk Limestone points to the presence of metasomatic processes. Merino and Banerjee (2008) stated that isovolumetric replacement could explain why RMS and karst are associated, since this process could transform a limited volume of limestone into considerable soil mass, and produces acids which lead to further leaching of the limestone. Thin sections of the rock–soil transition at the RMS on limestone near the village of Yarmouk confirmed the presence of partially replaced microfossils and thus the contribution of this process to the formation of the RMS at this location (Lucke et al., 2012). Based on the observed gradual change of the limestone under the RMS on silicified limestone near Irbid, we consider it possible that metasomatism is also active at this location. The great depth of some soil profiles on limestone, and possibly also on basalt, might be explained by this process. Other locations with few rock pores, like the Yarmouk caliche, might in contrast never have been affected by metasomatism.

However, it is unclear how the elementary ions driving the growth of clay minerals in the rock pores are supplied to the reaction front. Merino and Banerjee (2008) suggested that they are leached with aerosols, but in the light of high $CaCO_3$-values, for example in the RMS on limestone near the village of Yarmouk, it seems unlikely that the required elements would not precipitate before reaching the pores of the bedrock. As long as there is no other carrier or source of these elements, such as plant roots or ascending waters from the bedrock itself, it seems possible that the metasomatic features are relics. However, it could have been a strongly active process during moister climatic periods, such as the Pleistocene. Taimeh (1984) showed that a significant number of RMS in the vicinity of Irbid must have been completely de-calcified in the past, but were at some point re-calcified, which reversed the soil development and destroyed most clay films.

## 6. Conclusions

The distribution of Red Mediterranean Soils in Jordan requires a multi-causal explanation for their genesis. Comparing soils developed on basalt, sandstone, and limestone: in the first two bedrock types the important role of the primary lithology is clearly indicated by the element contents and bedrock fragments throughout the soil profiles. The Red Mediterranean Soils on limestone (Terrae Rossae), in contrast, are characterised by enrichment of montmorillonite, Zr, Ti, and to some degree Rb, Ba, Hf, W, Pb, Ce, and metal elements. Their formation seems, on the one hand, primarily related to the intensity of calcium carbonate leaching, which could be closely linked with bedrock porosity, and to some degree with metasomatic replacement processes. On the other hand, our study confirmed a similar element distribution across the investigated RMS on limestone and basalt and comparable mineralogical and chemical compositions, regardless of region, all of which points to at least one external source of soil parent material. This source is most likely connected with deposition of aerosols due to long-range and long-term dust transport from the Sahara, in particular from Sudan and Egypt.

Paleosols and initial soils developed on limestone Regolith of ancient ruins make clear that soil development was reduced during the Holocene, and that the character of aerosol deposition changed towards a greater share of silt — although the source region apparently remained the same. As proposed by Issar and Bruins (1983), this could be linked with a different precipitation pattern. The change of climate towards drier conditions is probably the major factor for the very limited soil development, in particular a lack of rubefication during the Holocene. Hence, Red Mediterranean Soils in Jordan might largely resemble the remains of a paleolandscape.

## Acknowledgements

This research was supported by a research grant by the German Research Foundation (DFG, grant nos. SCHM 2107/2-1, BA 1637/4-1) which we gratefully acknowledge. We would like to thank Robert Atkinson (BTU Cottbus) for a revision of the English grammar, and two anonymous reviewers for recommendations that helped to improve the manuscript.

## References

Bender, F., 1974. Geology of Jordan.Gebrüder Bornträger, Berlin.
Blanck, E., 1915. Kritische Beiträge zur Entstehung der Mediterran-Roterde. Die Landwirtschaftlichen Versuchsstationen LXXXVII, Berlin, pp. 251–314.
Blanck, E., 1926. Vorläufiger Bericht über die Ergebnisse einer bodenkundlichen Studienreise im Gebiet der südlichen Etschbucht und des Gardasees. Chemie der Erde 2, 175–208.
Boero, V., Schwertmann, U., 1987. Occurrence and transformations of iron and manganese in a colluvial Terra Rossa toposequence of northern Italy. Catena 14, 519–531.
Bronger, A., Bruhn-Lobin, N., 1997. Paleopedology of Terrae rossae — Rhodoxeralfs from Quaternary calcarenites in NW Morocco. Catena 28, 279–295.
Bronger, A., Ensling, J., Kalk, E., 1984. Mineralverwitterung, Tonmineralneubildung und Rubefizierung in TerraeCalcis der Slowakei. Catena 11, 115–132.
Cabadas, H., Solleiro, E., Sedov, S., Pi, T., Alcalá, J., 2010. The complex genesis of red soils in Peninsula de Yucatán, Mexico: mineralogical, micromorphological and geochemical proxies. Eurasian Soil Science 43 (13), 1439–1457.
Cabadas-Báez, H., Solleiro-Rebolledo, E., Sedov, S., Pi-Puig, T., Gama-Castro, J., 2010. Pedosediments of karstic sinkholes in the eolianites of NE Yucatán: a record of Lat Quaternary soil development, geomorphic processes and landscape stability. Geomorphology 122, 323–337.
Cordova, C., 2007. Millenial Landscape Change in Jordan. University of Arizona Press, Tucson.
Cornell, R., Schwertmann, U., 2003. The Iron Oxides.. Wiley VCH, Weinheim.
Danin, A., Gerson, R., Marton, K., Garty, J., 1982. Patterns of limestone and dolomite wheathering by lichens and blue-green algae and their paleoclimatic significance. Palaeogeography, Paleoclimatology, Paleaoecology 37, 221–233.
Delgado, R., Martín-García, J., Oyonarte, C., Delgado, G., 2003. Genesis of the terrae rossae of the Sierra Gádor (Andalusia, Spain). European Journal of Soil Science 54, 1–16.
DIN 19683, Deutsches Institut für Normung, 1973. Blatt 1–3, Physikalische Laboruntersuchungen, Bestimmung der Korngrößenzusammensetzung nach Vorbehandlung mit Natriumpyrophosphat. Beuth Verlag, Berlin.
DIN 51001, Deutsches Institut für Normung, 2003. Allgemeine Arbeitsgrundlagen zur Röntgenfluoreszenz-Analyse (RFA) sowie Beiblatt 1 (Uebersicht stoffgruppenbezogener Aufschlussverfahren zur Herstellung von Proben fuer die RFA). Beuth Verlag, Berlin.
Durn, G., Ottner, F., Slovenec, D., 1999. Mineralogial and geochemical indicators of the polygenetic nature of Terra Rossa in Istria, Croatia. Geoderma 91, 125–150.
El-Akhal, H., 2004. Contribution to the petrography, geochemistry, and tectonic setting of the basalt flows of the Umm–Quais plateau, north Jordan. Geological Bulletin of Turkey 47 (1), 1–11.
Eltayeb, M., Injuk, J., Maenhaut, W., Grieken, R., 2001. Elemental composition of mineral aerosol generated from Sudan Sahara Sand. Journal of Atmospheric Chemistry 40, 247–273.
Feng, J.-L., Zhu, L.-P., 2009. Origin of terra rossa on Amdo North Mountain on the Tibetan plateau, China: evidence from quartz. Soil Science and Plant Nutrition 55, 407–420.

Please cite this article as: Lucke, B., et al., Red Mediterranean Soils in Jordan: New insights in their origin, genesis, and role as environmental archives, Catena (2013), http://dx.doi.org/10.1016/j.catena.2013.04.006

ARTICLE IN PRESS



Ganor, E., 1975. Atmospheric dust in Israel: Sedimentological and Meteorological Analysis of Dust Deposition. PhD Thesis The Hebrew University of Jerusalem (in Hebrew with English abstract).
Ganor, E., Foner, A., 1996. The mineralogical and chemical properties and the behaviour of Aeolian Saharan dust over Israel. In: Guerzoni, S., Chester, R. (Eds.), The Impact of Desert Dust Across the Mediterranean. Kluwer Academic publishers, Dordrecht, pp. 163–172.
González Martín, J., Rubio Frnández, V., García Giménez, R., Jiménez Ballesta, R., 2007. Red palaeosols sequence in a semiarid Mediterranean environment region. Environmental Geology 51, 1093–1102.
Hurst, V., 1977. Visual estimation of iron in saprolite. Geological Society of America Bulletin 88, 174–176.
Israelevich, P., Levin, Z., Joseph, J., Ganor, E., 2006. Desert aerosol transport in the Mediterranean region as inferred from the TOMS Aerosol Index. http://geophysics.tau.ac.il/meidex/Publiations/Paper1/Paper1a.htm (In the Internet [2007-02-17]).
Issar, A.S., Bruins, H.J., 1983. Special climatological conditions in the deserts of Sinai and the Negev during the Latest Pleistocene. Paleogeography, Palaeoclimatology, Palaeoecology 43, 63–72.
Issar, A., Tsoar, C., Gilead, I., Zangvil, A., 1987. A paleoclimatic model to explain depositional environments during Late Pleistocene in the Negev. In: Berkofsky, L., Wurtele, G. (Eds.), Progress in Desert Research. Rowman& Littlefield, Totowa, pp. 302–309.
Jahn, R., 1995. Ausmaß äolischer Einträge in circumsaharische Böden und ihre Auswirkungen auf Bodenentwicklung und Standorteigenschaften. Hohenheimer bodenkundliche Hefte 23, Stuttgart.
Ji, H., Wang, S., Ouyang, Z., Zhang, S., Sun, C., Liu, X., Zhou, D., 2004a. Geochemistry of red residua underlying dolomites in karst terrains of Yunnan–Guizhou Plateau. I. The formation of the Pingba profile. Chemical Geology 203, 1–27.
Ji, H., Wang, S., Ouyang, Z., Zhang, S., Sun, C., Liu, X., Zhou, D., 2004b. Geochemistry of red residua underlying dolomites in karst terrains of Yunnan–Guizhou Plateau. II. The mobility of rare elements during wheathering. Chemical Geology 203, 29–50.
Khresat, S., Taimeh, A., 1998. Properties and characterization of vertisols developed on limestone in a semi-arid environment. Journal of Arid Environments 40, 235–244.
Krienitz, M.-S., Haase, K., Mezger, K., Shaick-Mashail, M., 2007. Magma genesis and mantle dynamics at the Harrat Ash Shamah volcanic field (southern Syria). Journal of Petrology 48 (8), 1513–1542.
Kubilay, N., Nickovic, S., Moulin, C., Dulac, F., 2000. An illustration of the transport and deposition of mineral dust onto the eastern Mediterranean. Atmospheric Environment 34, 1293–1303.
Lausser, P., 2010. Clay minerals as indicators for origin and age of Red Mediterranean Soils in Jordan. FAU Erlangen-Nuremberg (Unpublished Master Thesis).
Leiningen, W. Graf zu, 1915. Über die Einflüsse von äolischer Zufuhr für die Bodenbildung. Mitteilungen der Geologischen Gesellschaft zu Wien 7, 139–177.
Leiningen, W. Graf zu, 1930. Die Roterde (Terra Rossa) als Lösungsrest mariner Kalkgesteine. Chemie der Erde 4, 178–187.
Lucke, B., 2008. Demise of Decapolis. Past and Present Desertification in the Context of Soil Development, Land Use and Climate. Verlag Dr. Müller, Saarbrücken.
Lucke, B., Kemnitz, H., Bäumler, R., 2012. Evidence for isovolumetric replacement in some Terra Rossa profiles of northern Jordan. Boletin de la Sociedad Geológica Mexicana 64 (1), 21–35.
Merino, E., Banerjee, A., 2008. Terra rossa genesis, implications for karst, and eolian dust: a geodynamic thread. Journal of Geology 116, 62–75.
Meyer, B., 1979. Die Entcarbonatisierungsrötung als bodengenetischer Teilprozeß. Mitteilungen der deutschen bodenkundlichen Gesellschaft 29-II. 705–708.
Moh'd, B., 2000. The Geology of Irbid and Ash Shuna Ash Shamalia (Waqqas). Map Sheets No. 3154-II and 3154-II. Bulletin, 46. Natural Resources Authority, Geology Directorate, Geological Mapping Division, The Hashemite Kingdom of Jordan.
Molinaroli, E., 1996. Mineralogical characterization of Saharan dust with a view to its final destination in Mediterranean sediments. In: Guerzoni, S., Chester, R. (Eds.), The Impact of Desert Dust Across the Mediterranean. Kluwer Academic publishers, Dordrecht, pp. 153–162.
Moormann, F., 1959. The soils of East Jordan: Report to the government of Jordan (Expanded Technical Assistance Program No. 1132). FAO, Rome.
Moresi, M., Mongelli, G., 1988. The relation between the Terra Rossa and the carbonate-free residue of the underlying limestones and dolostones in Apulia, Italy. Clay Minerals 23, 439–446.
Muhs, D., 2001. Evolution of soils on Quaternary reef terraces of Barbados, West Indies. Quaternary Research 56, 66–78.
Muhs, D.R., Budahn, J., Prospero, J.M., Carey, S.N., 2007. Geochemical evidence for African dust inputs to soils of western Atlantic islands: Barbados, the Bahamas and Florida. Journal of Geophysical Research 112. http://dx.doi.org/10.1029/2005JF000445 F02009.
Muhs, D., Budahn, J., Avila, A., Skipp, G., Freeman, J., Patterson, D., 2010. The role of African dust in the formation of Quaternary soils on Mallorca, Spain and the implications for the genesis of Red Mediterranean soils. Quaternary Science Reviews 29, 2518–2543.
National Atlas of Jordan, 1984. Royal Geographic Centre of Jordan. National Atlas of Jordan, Part One. Agriculture and Climatology, Amman.
Nowell, A., Bisson, M., Cordova, C., 2003. Wadi al-Koum survey. American Journal of Archaeology 107, 453–455.
NSM&LUP, 1993. National Soil Map and Land Use Project. The Soils of Jordan. Level 1, Reconnaissance Soil Survey, Volume 2, Main Report. Amman Hashemite Kingdom of Jordan, Ministry of Agriculture, Hunting Technical Services Ltd., Soil Survey and Land Research Centre.
Prognon, F., Cojan, I., Kindler, P., Thirdy, M., Demange, M., 2011. Mineralogical evidence for a local volcanic origin of the parent material of Bermuda Quaternary paleosols. Quaternary Research 75, 256–266.
Reifenberg, A., 1927. Über die Rolle der Kieselsäure als Schutzkolloid bei der Entstehung mediterraner Roterden: Zeitschrift für Pflanzenernährung. Düngung, Bodenkunde 10, 159–186.
Reifenberg, A., 1947. The Soils of Palestine.T. Murby, London.
Retallack, G., 2001. Soils of the Past. An Introduction to Paleopedology. 2nd ed. Blackwell, London.
Rietveld, H., 2010. The Rietveld Method: a retrospection. Zeitschrift für Kristallographie 225, 545–547.
Rösner, U., Baumhauer, R., 1996. Paläoböden und Edaphoide basaltischen Ursprungs in Syrien — erste Ergebnisse tonmineralogischer Untersuchungen. Petermanns Geographische Mitteilungen 140, 227–235.
Ruhe, R., Olson, C., 1980. Clay-mineral indicators of glacial and nonglacial sources of Wisconsinan Loesses in southern Indiana, U.S.A. Geoderma 24, 283–297.
Schlichting, E., Blume, H.-P., Stahr, K., 1995. Bodenkundliches Praktikum. Wissenschafts-Verlag, Berlin.
Schmidt, M., Lucke, B., Bäumler, R., al-Saad, Z., al-Qudah, B., Hutcheon, A., 2006. The Decapolis region (Northern Jordan) as historical example of desertification? Evidence from soil development and distribution. Quaternary International 151, 74–86.
Schwertmann, U., Murad, G., Schulze, D.G., 1982. Is there holocene reddening (haematite formation) in soils of axeric temperature areas? Geoderma 27, 209–223.
Semmel, A., 1988. Rötliche Böden auf altpleistozänen Rheinterrassen. Berichte zur deutschen Landeskunde 62 (2), 357–369.
Shijie, W., Hongbing, J., Ziyuan, O., Deqan, Z., Leping, Z., Tingyu, L., 1999. Preliminary study on weathering and pedogenesis of carbonate rock. Science in China 42 (6), 572–581.
Sindowski, K.H., 1956. Sedimentpetrographisch- bodenkundliche Untersuchungen aneinigen Steppen-, Vollwüsten-, und Extremwüstenböden und Gesteinen aus der mittleren. In: Meckelein, W. (Ed.), Sahara (Lybien). Forschungen in der zentralen Sahara, pp. 152–179.
Singer, A., Danin, A., Zöttl, H., 1992. Atmospheric Dust and Aerosols as Sources of Nutrients in a Mediterranean Ecosystem of Israel. Bundesministerium für Forschung und Technologie.
Skowronek, A., 1978. Untersuchungen zur Terra rossa in E- und S-Spanien — ein regionalpedologischer Vergleich. Würzburger Geographische Arbeiten 47, Würzburg.
Stiles, C., Stensvold, K., 2008. Loess contribution to soils forming on dolostone in the driftless area of Wisconsin. Soil Science Society of America Journal 72 (3), 650–659.
Taimeh, A., 1984. Paleoclimatic changes during the Quaternary in the Irbid region. Dirasat XI (7), 131–149 (published by the University of Jordan).
Temur, S., Orhan, H., Deli, A., 2009. Geochemistry of the limestone of Mortas Formation and related terra rossa, Seydisehir, Konya, Turkey. Geochemistry International 47, 67–93.
U.S. Department of Agriculture, 2005. Keys to Soil Taxonomy9th edition. University Press of the Pacific, Honolulu, Hawaii.
WRB, 2007. World Reference Base of Soil Resources 2006, First Update 2007. World Soil Resources Reports No. 103. FAO, Rome.
Yaalon, D.H., Ganor, E., 1973. The influence of dust on soils during the quaternary. Soil Science 116 (3), 146–155.
Yaalon, D.H., Ganor, E., 1979. East Mediterranean trajectories of dust-carrying storms from the Sahara and Sinai. In: Morales, C. (Ed.), Saharan Dust: Mobilization, Transport, Deposition. Wiley, Chichester, pp. 187–196.
Zippe, W., 1854. Einige geognostische und mineralogische Bemerkungen über den Höhlenkalkstein des Karst. In: Schmidl, A. (Ed.), Die Grotten und Höhlen von Adelsberg, Lueg, Planina und Laas: Wien, pp. 209–221.

Please cite this article as: Lucke, B., et al., Red Mediterranean Soils in Jordan: New insights in their origin, genesis, and role as environmental archives, Catena (2013), http://dx.doi.org/10.1016/j.catena.2013.04.006